UNIVERSIDADE DE LISBOA
FACULDADE DE CIÊNCIAS
DEPARTAMENTO DE ENGENHARIA GEOGRÁFICA, GEOFÍSICA E ENERGIA

Improvement of a physiological human model

Carlos Manuel Ferreira Domingos

Mestrado Integrado em Engenharia da Energia e do Ambiente

2014

UNIVERSIDADE DE LISBOA
FACULDADE DE CIÊNCIAS
DEPARTAMENTO DE ENGENHARIA GEOGRÁFICA, GEOFÍSICA E ENERGIA

Improvement of a physiological human model

Carlos Manuel Ferreira Domingos

Dissertação de Mestrado em Engenharia da Energia e do Ambiente

Trabalho realizado sob a supervisão de:

Dr.-Ing. Rita Streblow (RWTH)

Dr. Eng. Guilherme Carrilho da Graça (FCUL)

2014

Abstract

At the institute for Energy Efficient Buildings and Indoor Climate the 33 node thermal comfort model (33NCM) was developed for the analysis of inhomogeneous indoor environments. The model can be separated into a physiological model, which calculates the thermal body state and a psychological model which calculates the thermal sensation and comfort based on the thermal body state. The model can be used as stand-alone or in coupled mode with computational fluid dynamics (CFD) calculations of the thermal boundary conditions indoors.

The master thesis has its focus on the physiological model programmed in Modelica. From a literature review data sets for model validation was extracted. From the data analysis and the model testing an approach for the model improvement was developed. The usability and stability of the model were improved, e.g. through the integration of records, perspiration and a redraft of if-statements. The results were summarized to be usable for a validation manual. The model improvements were finally integrated in a coupled simulation between the comfort model and a CFD calculation for a small computational domain with one person. For different boundary conditions the model stability was checked.

Resumo

No instituto de Eficiência Energética em Edifícios e Climatização, foi desenvolvido o modelo de conforto térmico de 33 nós (33 NCM) para análise de ambientes heterogéneos internos. O modelo pode ser separado num modelo fisiológico, o qual calcula o estado térmico do corpo, e num modelo psicológico, que calcula a sensação e conforto térmico com base no estado térmico do corpo. O modelo pode ser usado isoladamente ou em conjunto com cálculos de dinâmica de fluidos computacional (CFD), do inglês "Computacional Fluid Dynamics" das condições térmicas de fronteira em ambientes no interior.

A tese de mestrado tem o seu foco no modelo fisiológico, programado em Modelica. A partir da revisão bibliográfica extrairam-se dados para validação do modelo. Através da análise destes e do teste do modelo foi desenvolvida uma nova abordagem para a melhoria do modelo. A usabilidade e a estabilidade do modelo foi melhorada, por exemplo, através da integração de registos e de uma reformulação das condições “if’s”. Os resultados foram resumidos para a realização de um manual de validação. As melhorias do modelo foram finalmente integradas numa simulação que inclua o modelo de conforto e o cálculo de CFD para um pequeno domínio computacional com uma pessoa. Para diferentes condições fronteira a estabilidade do modelo foi verificada.

Acknowledgements

I would like to thank all my colleagues, friends, family and my girlfriend that I met along the path of my studies.

In particular and first of all, I would like to thank Dr.-Ing. Rita Streblow for the precious advices, patience and support she gave me during our meetings and for providing an excellent atmosphere for my research. She has been a teacher for me, and she helped me to grow in a scientific way. Then I would like to thank Dr. Eng. Guilherme Carrilho da Graça, he was the reason that I chose this field of work, he was a huge inspiration.

I would like to thank Frank Tilger, who was a good friend and it would have been a lonely office without him. I would also like to thank him for having given me the chance to join his soccer team. I am really grateful to him since it was a wonderful experience. I met beautiful people and this helped me to feel a bit more like home. Many thanks to Niklas Paparott, Dawid Nickel, Jan Reinhardt, Marcel Nebeling, Konstantin Finkbeiner and all other students in the E.ON Energy Research Center that helped me and were great companions.

Special thanks to my former colleagues at Faculdade de Ciências da Universidade de Lisboa, where I did all my courses. Special thanks to Rodrigo Silva, Isaac Afonso and Rita Almeida, I would not have been able to accomplish my degree without these friends. They helped my during all my five years of study. Thanks to Miguel Vargues, João Cristóvão, Daniel Martins, João Dias, Pedro Fortes, Maria Inês and many other colleges that I had during my studies. All these friends and colleagues helped me to grow as a student and person.

I would also like to express my sincere gratitude to my parents, my elder brother and all my family. They were always supporting me and encouraging me with their best wishes.

Last, but by no means least, I would like to thank my girlfriend, Catarina Nunes. She was always there cheering me up and stood by me through the good and bad times.

Contents

Glossary

Symbol and Unit

Symbol	Description	Unit
A	Area	m^2
a	Ratio of counter current heat transfer	JK^{-1}
AH	Absolute humidity	gm^{-3}
B	Heat exchange rate between central blood compartment and node	W
BF	Blood flow rate	ls^{-1}
BFB	Basal blood flow rate	ls^{-1}
b	Coefficient Reynolds number	
C	Coefficient Reynolds number	
C_{ch}	Shivering control coefficient for core layer of head segment	WK^{-1}
C_d	Thermal conductance	WK^{-1}
C_{Dl}	Vasodilation control coefficient for core layer of head segment	$lh^{-1}K$
C_h	Heat production by shivering	W
C_p	Heat Capacity	JK^{-1}
C_{St}	Vasoconstriction control coefficient for core layer of head segment	K^{-1}
C_{Sw}	Sweat control coefficient for the core layer of head segment	WK^{-1}
$Chilf$	Distribution coefficient of core layer for shivering heat production	
Cld	Cold signal	K
Clds	Integrated cold signal	K
CSF	Surface area rate in contact with external object	
D	Conductive heat exchange rate with neighbouring layer	W
D_{AB}	Binary mass diffusivity	m^2s^{-1}
D_l	Vasodilation signal	ls^{-1}
d	Characteristic dimension	m

continued on next page

Symbol and Unit

Symbol	Description	Unit
E	Evaporative heat loss at skin surface	W
E_b	Water vapor diffusion through the skin	W
E_{sw}	Evaporation of insensible sweat	W
E_{max}	Maximum evaporative heat loss	W
Err	Error signal	K
f_{cl}	Clothing correction factor	
h_c	Convective heat transfer	$Wm^{-2}K^{-1}$
h_e	Evaporative heat transfer	$Wm^{-2}K^{-1}$
h_r	Radiative heat transfer	$Wm^{-2}K^{-1}$
I_{cl}	Intrinsic clothing resistance	clo
i_{cl}	Vapour permeation efficiency of clothing	
K	Coefficient convective heat transfer	
k	Thermal conductivity	$Wm^{-1}K^{-1}$
km	Local multiplier	
LR	Lewis ratio	
M	Molar mass	$kgmol^{-1}$
MST	Mean Skin Temperature	°C
met	Metabolic rate	W
Met_f	Distribuition coefficient of a core layer of heat production by external work	
n	Coefficient convective heat transfer	
Nu	Nusselt number	
P	Pressure	Nm^{-2}
P_{Ch}	Shivering control coefficient for the core layer of head segment and the skin layer of each segment	WK^{-2}
P_{Dl}	Vasodilation control coefficient for the core layer of head segment and skin layer of each segment	$lh^{-1}K^2$
P_{St}	Vasoconstriction control coefficient for core layer of head segment and skin layer of each segment	K^{-2}
P_{Sw}	Sweat control coefficient for signals from core layer of head segment and skin layer of each segment	WK^{-2}

continued on next page

Symbol and Unit

Symbol	Description	Unit
Q	Rate of heat production	W
Q_b	Basal metabolic rate	W
Q_c	Heat losses through convection	W
Q_e	Heat transfer through evaporation	W
Q_{mt}	Heat transfer by conduction	W
Q_r	Heat losses through radiation	W
Q_s	Gains due to solar radiation	W
Q_t	Convective and radiant exchange rate between skin surface and environment	W
R	Universal gas constant	$JK^{-1}mol^{-1}$
Re	Reynolds number	
RES	Heat loss by respiration	W
SC	Sutherland's constant	
S_{Ch}	Shivering control coefficient for skin layer of each segment	WK^{-1}
S_{Dl}	Vasodilation control coefficient for skin layer of each segment	$lh^{-1}K$
S_{St}	Vasoconstriction control coefficient for skin layer of each segment	K^{-1}
S_t	Vasoconstriction signal	
S_{Sw}	Sweat control coefficient for skin layer of each segment	WK^{-1}
SKINC	Distribution coefficient of the skin layer for S_t	
SKINR	Weighting coefficient for integration of sensor signal	
SKINS	Distribution coefficient of the skin layer for sweat	
SKINV	Distribution coefficient of the skin layer for D_l	
T	Temperature	°C
v	Velocity	ms^{-1}
W_t	Weight	kg
W	Heat production by external work	W
Wrm	Warm signal	K
Wrms	Integrated warm signal	K

Greek Symbols

Symbol	Description	Unit
α	Thermal diffusivity	$\mathrm{m}^2 s^{-1}$
ε	Emissivity	
μ	Dynamic viscosity	Pas
ρ	Mass density	kgm^{-3}
σ	Stefan-Boltzmann constant	$Wm^{-2}K^{-4}$
τ	Temperature in degrees Rankine	$^\circ R$
υ	Kinematic viscosity	$m^2 s^{-1}$
ϕ	Relative humidity	

Indices and Abbreviations

Symbol	Description
a	Ambient
ab	Abdomen
cl	Clothes
c	Convection
cr	Core
d	Dry air
e	Evaporative
f	Forced
h	Head
in	Initial
m	Mixed
mn	Mean
n	Natural (free)
r	Radiation
rsp	Respiration
s	solar
sk	Skin
sum	Sum

continued on next page

Indices and Abbreviations

Symbol	Description
v	Saturated water vapour

List of Figures

List of Tables

1 Introduction

Humans as living organisms must be in thermal balance with their environment in order to survive. Human thermal response, perceived as thermal comfort or discomfort, is dependent by four environmental parameters: air temperature and speed, radiant temperature and relative humidity; and two personal variables: the metabolic human heat by activity and the clothings insulation [Spengler et al., 2000].

This thesis concerns on the improvement of an existing physiological human model of the 33 Node Comfort Model (33NCM) developed out by Rita Streblow at the RWTH Aachen University, E.ON Energy Research Center, Institute for Energy Efficient Buildings and Indoor Climate [Streblow, 2011].

The 33NCM is programmed in the object oriented programming language Modelica. The model was calibrated with own experimental data covering a temperature range of typical indoor environments. Under more extreme conditions the model showed less precise data. With a comparison to different test cases from the literature the model could be improved especially with a temperature dependent formulation of some parameters.

In section 5 creates a manual validation for the 33 NCM, in which the 33 NCM was always compared with some measurements from the literature or with other models, to validate the improvements made.

Was also calculated in a coupled mode with numerical flow simulation (CFD). In this case a cycle is created, where the radiative and convective heat transfer coefficients are replaced by values that come from the CFD, and the temperatures from the 33 NCM go back to the CFD, to calculate again the cycle.

1.1 State of the art

Fanger [1970] developed the most widely used model for the evaluation of indoor environments which is also integrated into the standards. He calculates the Predicted Mean Vote (PMV), which is derived from the physics of heat transfer combined with an empirical fit to sensation, and the Predicted Percentage Dissatisfied (PPD), which is based on a human body discretized a one compartment under steady state conditions. While the base work was systematic to research the indoor thermal comfort conditions, their purpose was to reach the perfect thermal environment and find

a correlation to mean values of radiant temperature, air temperature, air velocity and humidity. Although this is a good approach , it is not adequate for the evaluation of thermal comfort in buildings, where more precise.

Soon after in the next year Stolwijk and B. [1971] developed a more complex model with single body segments. On this work several other developments are based. Beside others Arkin and Shitzer [1984] developed two different parts, which differentiate between a passive and active model. Years after, Fiala [1998] developed a model in 1998 to predict human thermal responses and the associated thermal sensation in a wide range of environments. Also based on the Stolwijk model, Tanabe et al. [2002] developed a model which differentiates between sixteen body parts. Together with four body layers and a central blood compartment it gives a 65 multi node model. Later on, he improved and simplified the Tanabe model [Murakami et al., 2007]. Besides the Fanger model, all aforementioned models differ in their level of detail, but they all describe the physiological human body behaviour. One of the calculated outputs is the human body temperature. Zhang [2003] developed a psychological model which calculates based on the physiological thermal body state, the local thermal sensation as a voting for warm, cold and the local thermal comfort as a voting for comfortable or uncomfortable. From both measures the global sensation and comfort is calculated. Based on the Tanabe and Zhang model, Streblow [2011] developed the 33 NCM which is simplified compared to the Tanabe model but still resolving 16 different body parts.

Table 1.1 gives an overview about theses comfort models.

1.2 Commercial tools

The commercial tools that presently exist are all based on two models, the Fiala model [Fiala, 1998] and ASHRAE model [ASHRAE, 2013]. The ASHRAE model is a simplified model and cannot be directly compared with Fiala or 33 NCM, because is no complex physiological model behind. This model works by specifying a combination of personal and indoor thermal environmental factors which in turn results in thermal environmental conditions acceptable for most of the occupants within a certain space. This is a more general and simple model, where different parameters need to be defined step-by-step, such as each person's metabolic activity and clothing, in order to discover a thermal environment that is acceptable for almost all occupants. However, this standard only addresses thermal comfort considering steady state conditions.

THESEUS-FE created a professional tool called *THESEUS-FE*, based on the Fiala model which can be used for fully transient and steady-state thermal applications, e.g. studies of passenger comfort in the complete cabin interior. This tool is mainly used for the transportation sector such as the automotive or aerospace industry, but is also applicable for other markets [THESEUS-FE].

XRG Simulation GmbH created the *HumanComfort* Modelica library, based on the ASHRAE model, which contains models that allow a mathematical evaluation of thermal comfort. With this library, analysis can be made in order to examine how air conditioning failure affects human comfort, by simultaneously simulating the building and the air conditioning. Thus, this library supports the excellent control of an air conditioning system [XRG Simulation GmbH].

The *ThermoAnalytics* human comfort module based on the Fiala model is an advanced plug-in for the analysis of human thermal comfort within complex environments that can be used for indoor or outdoor cases and for transportation systems. The human comfort plug-in for *RadTherm* and *MuSES* software allows for the user to run simulations of virtual manikins in these environments returning their comfort indexes as an output. Each manikin is composed by different body parts and also allows the use of different types of clothing in different body parts [ThermoAnalytics, Inc.].

ASHRAE's Thermal Comfort Tool software provides a user-friendly interface, for calculating thermal comfort parameters and making thermal comfort predictions. This model is based on several existing thermal comfort models [THESEUS-FE, 2012].

LumaSense Technologies has developed the *Thermal Comfort Manager Software-INNOVA 7701* based on the ASHRAE model. This software requires with a data logger which eases the data collection, by automatically storing measurements and allowing later on transferring the data to a computer, and consequent analysis of thermal comfort result [LumaSense Technologies].

1.3 33 NCM

The 33 NCM is developed to examine thermal comfort in complex non-uniform environments. As an example for a non-uniform case the special case of an airplane cabin was considered for the model development. The 33 NCM relates local thermal sensation and comfort to skin temperatures, which are defined by a physiological model. 16 single body parts are resolved and their local thermal sensation and comfort is transformed into an overall thermal sensation and comfort vote [Streblow, 2011].

1.4 Data for model development

For improvement and validation of the 33 NCM different data from the literature are used. All the test cases used within this work are described in chapter 5. Unfortunately not all boundary conditions are always well documented in literature so that in some cases additional assumptions for e.g. radiant temperature... had to be made.

For the validation of the pure passive system a dead man test case is used [THESEUS-FE, 2012]. In this case all mechanism of the active part (perspiration, shivering and vasomotion) are turned off.

The validation of the purely passive systems is followed by the validation of thermal neutrality, taking two different case studies in account. Firstly, a naked person is considered, where instead of comparing the 33NCMwith measurements, it is compared to other two models ([Fiala, 1998] and [THESEUS-FE, 2012]). Lastly, a clothed person is considered, where a comparison is made between experiment from Fiala [1998] and 33 NCM.

Once the thermal neutrality, had been validated, it was followed by a deeper analysis of the active system. This is the major part, where we begin with extreme conditions e.g. cooling environment at 5°C, and end with changing thermal boundary conditions e.g. 30-48-30 °C.

Table 1.1: Thermal comfort models [THESEUS-FE]

	Fanger [1970] PMV-Index	**Fiala [1998] DTS-Index**	**Assessment of equivalent temperatures (EN ISO 14505-2)**	**Zhang [2003] Local comfort model**	**33 NCM from Streblow [2011]**
Input	activity level global boundary cond.: air-and wall temperature, air -velocity, humidity clothing	mean skin temperature core temp.	local heat loss values	local skin temperature mean skin temperature core temperature	activity level global boundary cond.: air temperature, air -velocity, humidity clothing
Validity	stationary, global	dynamic, global	stationary, local + global, 6 assessment regions	dynamic, local + global, 13 body parts	dynamic, local + global, 16 body parts
Remarks	stand alone with thermal manikin response	DTS only valid for dynamic	different assessment for summer and winter clothing	model also provides max. thermal comfort value ⇒ applicable for optimization	can not change the weight
Handicap	not applicable for contact boundary conditions model requires global cloth. definition (clo-value)	less validated for dynamic load class	compared with Zhang: local comfort predictions are quite undifferentiated	very complex model results sometime not transparent ("black box")	limited validation from dynamic behaviour
Output (Indices)	global therm. sensation on a 7-step-scale -3 .. cold -2 .. cool -1 .. slightly cool 0 .. neutral +1 .. slightly warm +2 .. warm +3 .. hot		local therm. sensation and comfort on a 5-step-scale 1 .. too cold (uncomfort.) 2 .. cold (but comfort.) 3 .. neutral (comfortable) 4 .. warm (but comfort.) 5 .. too warm (uncomfort.)	global and local therm. sensation on a 9-step-scale from -4 (very cold) to +4 (very hot) thermal comfort on a 9-step-scale, from -4 (very uncomfortable) to +4 (very comfortable)	Overall and local Thermal sensation and comfort is provided via the 7-point ASHRAE scale with the limits +3 and -3

2 Human physiology

2.1 Introduction

It is crucial to keep the human body's core temperature at 37 °C, to ensure the good behaviour and function of the brain and inner organs. Only the skin temperature can vary in a wider temperature range depending on the different control mechanism of the human body.

Two systems can be clearly separated which give the human body the possibility to control its temperature. The first is the passive system, which causes heat to flow from the human body to the environment because of differences in temperature and water vapour pressure. The second system responsible for human thermoregulation is the active system with its actively controlled body mechanisms reacting to thermal challenges. Both systems together form a homoeostatic mechanism that keeps the human body temperature at a roughly constant level, regardless of the ambient temperature [Streblow, 2011].

2.2 Passive System

The heat balance of the passive system accounts for local heat losses from body parts. In this thesis the effects of free and forced convection are considered in more detail by considering heat and mass transfer through non-uniform clothing, long-wave radiation exchanges with surrounding surfaces and evaporation of moisture from the skin. However, not only these exchanges occur but also between the environment and the human surface skin or between parts of the body itself, which can be seen more in detail in fig. 2.1.

2.2.1 Convection

Convection is heat transfer by mass motion of a fluid when the heated fluid is caused to move away from the source of heat, carrying energy with it. Three different processes exist: free, mixed and forced convection. In free convection fluid motion is due to buoyancy, only dependent of temperature gradient, and generally confined to ambient air speeds lower than 0.2 ms^{-1}. *Buoyancy is an upward force exerted by a fluid that opposes the weight of an immersed object.* Mixed convection is

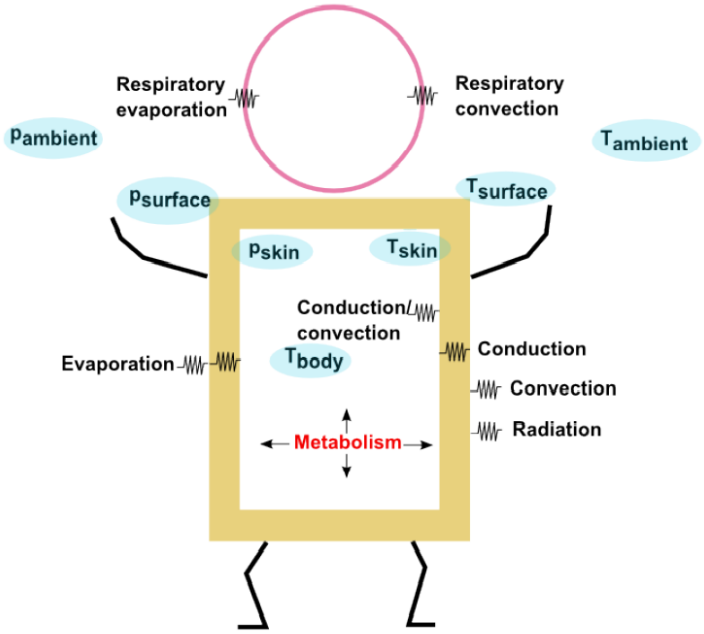

Figure 2.1: Heat loss mechanisms of the passive system from [Streblow, 2011]

a combination of forced and free convection, normally between $0.2 < v < 1.5\ ms^{-1}$. Forced convection is a mechanism, or type of transport in which fluid motion is generated by an external source, and depend only velocity, normally higher than $1.5\ ms^{-1}$.

2.2.2 Radiation

Radiation is energy that comes from a source and carries energy away from the emitting object in the form of electromagnetic wave, through some material or space. All Matter with a temperature greater than absolute zero emits thermal radiation, heat transfer by thermal radiation requires no matter.

2.2.3 Evaporation

Because of the large heat amount of vaporization of water, the evaporation from a liquid surface is a very effective cooling mechanism. The human body makes use of evaporative cooling by perspiration to give off energy even when surrounded by a temperature higher than body temperature. If part of a liquid evaporates, it cools the liquid remaining behind because it must extract the necessary heat of vaporization from that liquid in order to make the phase change to the gaseous state.

2.3 Active system

The active system of the body includes the thermoregulation specification of the passive system described in section 2.2. The active system does not change the nature of the heat transfer model. The dynamic active system of thermoregulation mechanism regulates the passive system. These two models must to be linked together into an integrated model, to be able that the overall system works. In this thesis the focus is on the sweat system, but the active system has also two more important mechanisms like shivering and vascular system, as it can be seen in fig. 2.2.

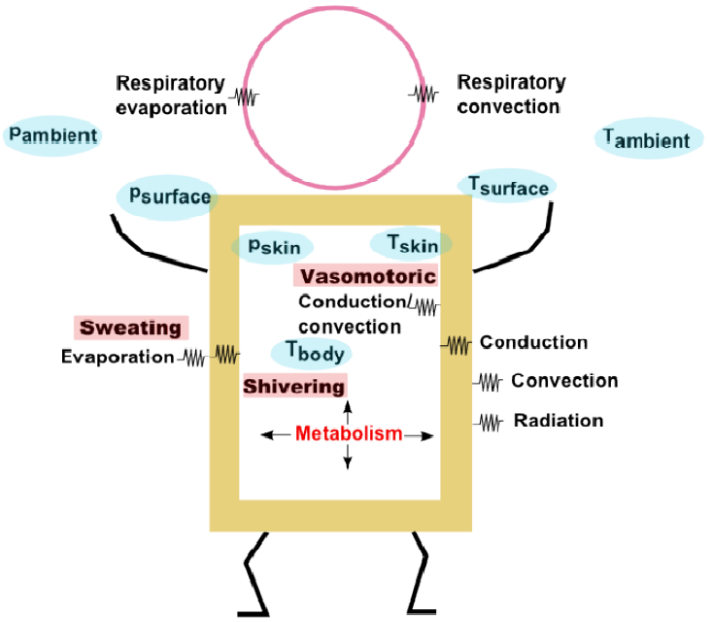

Figure 2.2: Heat loss mechanisms of the active system from [Streblow, 2011]

2.3.1 Sweating

Sweating is a body function that helps to regulate the body temperature. This is the most effective regulatory mechanism for dealing with a heat stress or body physical exercise, sweating is the release of a salty liquid from the body's sweat glands. When the temperature of the environment is higher than the skin, the sweat is the only mechanism capable to remove heat loss.

2.3.2 Shivering

Shivering is the most effective regulatory mechanism to increase the metabolic heat production to offset the cold stresses. Increased muscle activity (contract at high frequency), results in the generation of heat production above the basal level. This defence mechanism against cold stresses, serves the purpose to maintain the core temperature thermally comfortable [Arkin and Shitzer, 1984].

2.3.3 Vascular system

The vascular system besides to transport nutrients and waste products, also produces changes in the body's thermal resistance. The vasodilation have one of the purpose to increase the availability of heat transfer from the skin to the environment. In cold environments, the blood flow can be reduced down to a basic supply volume just sufficient for transporting oxygen to the cells [Streblow, 2011].

3 33 Node Comfort Model (33NCM)

This chapter is all based in:

“THERMAL SENSATION AND COMFORT MODEL FOR INHOMOGENEOUS INDOOR ENVIRONMENTS"

Author: Rita Streblow

The 33 NCM helps to answer numerous questions on the effect of different environments on thermal comfort. It provides information that can help to design and evaluate air-conditioning systems under the aspect of saving energy without cutting back on thermal comfort [Streblow, 2011].

3.1 33-node thermoregulation model

The physiological model was based on the Tanabe [Tanabe et al., 2002] and JOS models. The 33 NCM represents the anthrometric data of an average man with the body surface area of 1.868 m^2, and the body weight of 74.43 kg. The entire body is divided into 16 segments - Head, Chest, Pelvis, right and left Shoulders, right and left Arms, right and left Hands, right and left Thighs, right and left Legs, and right and left Feet; the subscript $i(= 1-16)$ represents the segment number in the following equation and the subscript $j(= 1-2)$ represents the core and the skin layer respectively. Surface area for each body part are shown in table 3.1, the weight is not discriminated. In addition, the 33 NCM has a central blood compartment, making a total of 33-nodes. The conceptual figure of the 33 NCM is illustrated in fig 3.1.

Heat is transferred through the tissues within individual segments by conduction. Heat exchange between local tissues and blood flow by convection.

3.2 human physiology

The body and the environment exchange heat by respiration, evaporation, radiation and convection.

For the convective and radiative heat transfer coefficients, the 33 NCM model used a study from de Dear et al. [1997], a thermal manikin composed of 16 body segments to generate radiative h_r and

Table 3.1: Surface area of numerical manikin [Streblow, 2011]

i	$Segment$	$Area[m^2]$
1	Head	0.120
2	Chest	0.140
3	Back	0.161
4	Pelvis	0.221
5	Right Shoulder	0.060
6	Left Shoulder	0.060
7	Right Arm	0.035
8	Left Arm	0.035
9	Right Hand	0.016
10	Left Hand	0.016
11	Right Thigh	0.200
12	Left Thigh	0.200
13	Right Leg	0.089
14	Left Leg	0.089
15	Right Foot	0.056
16	Left Foot	0.056
	Total	1.553

convective h_c heat transfer coefficients in $[Wm^{-2}K^{-1}]$(and limited to a seated person), to be used directly with the 33 NCM as shown in table 3.2.

For the evaporative heat transfer coefficient h_e from the skin surface to the environment, expressed as a function of clothing vapour permeation efficiency by equation 3.1.

$$h_{e,i} = \frac{LRi_{cl,i}}{0.155I_{cl,i} + i_{cl,i}/h_{c,i}f_{cl,i}} \tag{3.1}$$

LR is the Lewis Ratio and was used as a constant of 16.5, I_{cl} is the intrinsic clothing resistance in [clo], i_{cl} is the vapor permeation efficiency of clothing and the f_{cl} is the clothing correction factor [Kobayashi and Tanabe, 2013]. In this equation was also found a little mistake, besides the constant the $f_{cl,i}$ must to have a relative with $h_{c,i}$ like shown in equation 4.19.

3.3 Physiological passive model

3.3.1 Heat balance equations of the 33 NCM

The heat balance equation in two layers and central blood compartment are the following:

Core layer:

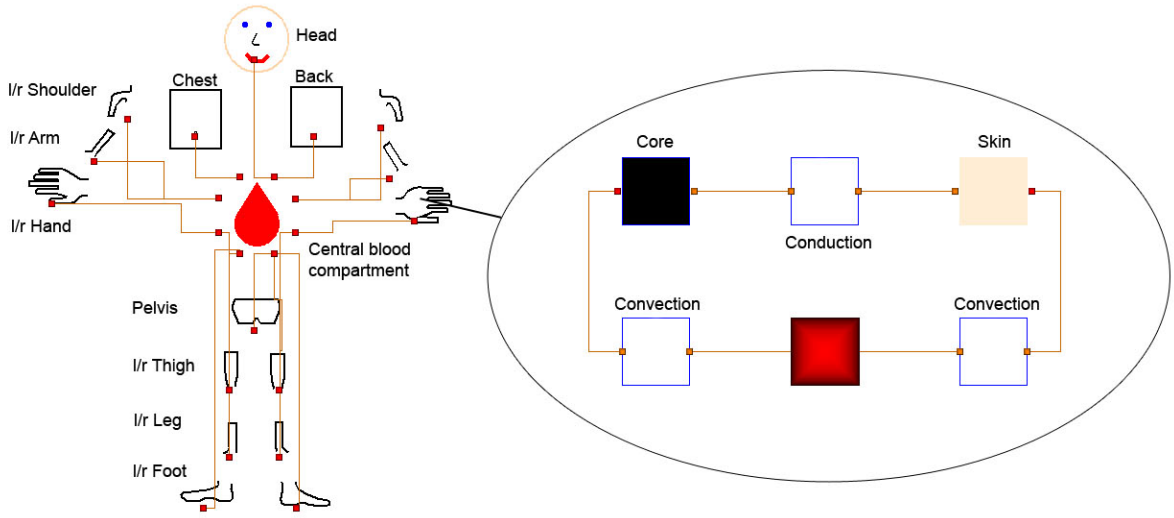

Figure 3.1: Conceptual figure of 33 NCM [Streblow, 2011]

$$C_{p,i,cr}\frac{dT_{i,cr}}{dt} = Q_{i,cr} - B_{i,cr} - D_i - RES_{i,cr} \tag{3.2}$$

Skin layer:

$$C_{p,i,sk}\frac{dT_{i,sk}}{dt} = Q_{i,sk} - B_{i,sk} - D_i - Q_{t,i,sk} - E_{i,sk} \tag{3.3}$$

Central Blood:

$$C_{p,33}\frac{dT_{33}}{dt} = \sum_{i=1}^{16}\sum_{j=1}^{2} B_{i,j} \tag{3.4}$$

Each term in these equations is described in the following subsections.

3.3.2 Heat capacity and heat production

$C_{p,i,j}$ is the heat capacity in [JK^{-1}] of node (i,j) and shown in table 3.3.

$T_{i,j}$: is the temperature in °C, $Q_{i,j}$ is the rate of heat production in [W] expressed by equation 3.5, and is the sum of basal metabolic rate $Qb_{i,j}$ in [W], heat production by external work $W_{i,cr}$ in [W], and heat production by shivering $Ch_{i,cr}$ in [W]. Heat production by external work and shivering only occur in the core layer. Basal metabolic rate of each node is shown in table 3.3. $METf_i$ is the distribution coefficient of core layer for heat production by external work.

Table 3.2: Body segment convective and radiative heat transfer coefficients for seated position [Streblow, 2011]

$Bodysegment$	$h_c[Wm^{-2}K^{-1}$ $v<0.1ms^{-1}$	$h_c[Wm^{-2}K^{-1}$ $v>0.1ms^{-1}$	$h_r[Wm^{-2}K^{-1}$
Head	3.7	$4.9v^{0.73}$	3.9
Chest	3.0	$9.4v^{0.59}$	3.4
Back	2.6	$8.9v^{0.63}$	4.6
Pelvis	2.8	$8.2v^{0.65}$	4.8
Shoulder	3.4	$11.2v^{0.62}$	4.8
Arm	3.8	$11.6v^{0.62}$	5.2
Hand	4.5	$12.6v^{0.60}$	3.9
Thigh	3.7	$8.9v^{0.60}$	4.6
Leg	4.0	$12.9v^{0.59}$	5.4
Foot	4.2	$12.8v^{0.55}$	4.2
Whole body	3.3		4.5

$$Q_{i,j} = Qb_{i,j} + W_{i,cr} + Ch_{i,cr} \tag{3.5}$$

$$W_{i,cr} = 58.2\,(met - Qb)\,AMETf_i \tag{3.6}$$

where A is the area of the skin and met is the metabolic rate in [met], what is wrong because Q_b is in [W], and improved in equation 4.35.

3.3.3 Heat transfer by blood flow

Equation 3.7 is the heat exchanged between each node and central blood compartment in [W]. where $a_{i,cr}$ is the ratio of counter-current heat exchange for the skin layer in $[JK^{-1}]$ and assumed that is included in the optimization process, lies between 0.5 and 1 in the hands and feet. It is further assumed that 80% of the arms and legs, and 70% of the correction coefficient are reached to the shoulders and thighs. ρC is the volumetric specific heat of blood ($\rho C = 1.067[WhK^{-1}]$) and BF_i is the blood flow rate in $[ls^{-1}]$ expressed in equation 3.8 for the core layer. T_{33} is the blood temperature the central compartment.

$$B_{i,j} = a_{i,cr}\rho CBF_i\left(T_{i,j} - T_{33}\right) \tag{3.7}$$

$$BF_{i,cr} = BFB_{i,cr} + \frac{W_{i,cr} + C_{h,i,cr}}{1.16} \tag{3.8}$$

Table 3.3: Heat capacity, basal metabolic rate and distribution coefficient by external work [Streblow, 2011]

	$C_{p,i}[WhK^{-1}$		$Q_{b,i,j}$		**MET** f_i
Segment (i)	**Core**	**Skin**	**Core**	**Skin**	
Head	2.1220	0.2200	16.8960	0.1040	0.000
Chest	10.2975	0.4410	24.2870	0.1790	0.091
Back	9.3935	0.4060	21.7370	0.1580	0.080
Pelvis	13.8340	0.5560	12.2910	0.2540	0.129
Shoulder	1.6994	0.1260	1.2150	0.0500	0.026
Arm	1.1209	0.0840	0.3460	0.0260	0.014
Hand	0.1536	0.0880	0.0900	0.0500	0.005
Thigh	5.3117	0.3340	1.3180	0.1220	0.201
Leg	2.8670	0.1690	0.3570	0.0230	0.099
Foot	0.2097	0.1070	0.2120	0.1000	0.005
Central blood		2.61			

Where $BFB_{i,j}$ is the basal blood flow rate and values used in the 33 NCM model are shown in table 3.4. It was assumed that a blood flow of 1.0 lh^{-1} was required for 1.16W heat production.

Table 3.4: Thermal conductance and basal blood flow rate [Streblow, 2011]

Segment	**Thermal condutance** WK^{-1}	Basal blood flow ratelh^{-1}	
		core	skin
Head	3.422	32.228	5.725
Chest	1.785	89.214	1.967
Back	1.643	87.663	1.475
Pelvis	2.251	33.518	2.272
Shoulder	1.501	1.808	0.910
Arm	0.982	0.940	0.508
Hand	2.183	0.217	1.114
Thigh	2.468	1.406	1.456
Leg	1.326	0.164	0.651
Foot	3.370	0.080	0.934

3.3.4 Heat exchange by conduction

D_i is the heat transmitted by conduction from the skin to the core layer in [W] within the same segment and is expressed by equation 3.9. $C_{d,i,j}$ is the thermal conductance in $[WK^{-1}]$ between the skin and the core layer. The values shown in table 3.4 were used in the 33 NCM model.

$$D_{i,j} = C_{d,i,j}\left(T_{i,cr} - T_{i,sk}\right) \tag{3.9}$$

3.3.5 Heat loss by respiration

The heat loss by respiration RES in [W] is supposed to occur only in the core layer of the chest segment node (2,1). $RES_{2,1}$ is expressed by equation 3.10.

$$RES_{2,1} = \left(0.0014\left(34 - T_{a,1}\right) + 0.017\left(5.867 - p_{a,1}\right)\right)\sum_{i=1}^{16}\sum_{j=1}^{2} Q_{i,j} \tag{3.10}$$

where $T_{a,1}$ and $p_{a,1}$ are air temperature and vapor pressure (in [°C] and [Pa]) at the head segment, respectively.

3.3.6 Evaporative heat loss at skin surface

$E_{i,cr}$ is evaporative heat loss in [W] at the skin surface and is expressed by equation 3.11. $E_{b,i,sk}$ is the heat loss by water vapor diffusion through the skin in [W]. The skin diffusion is assumed to 6% of $E_{max,i}$, as shown in equation 3.12. $E_{sw,i,sk}$ is the heat loss by evaporation of sweat in [W].

$$E_{i,sk} = E_{b,i,sk} + E_{sw,i,sk} \tag{3.11}$$

$$E_{b,i,sk} = 0.06\left(1 - \frac{E_{sw,i,sk}}{E_{max,i}}\right)E_{max,i} \tag{3.12}$$

$$E_{max,i} = h_{e,i}\left(p_{sk,i} - p_a\right)A_i \tag{3.13}$$

$p_{sk,i}$ is the saturate vapour pressure on the skin surface, and A_i is the surface area of the body segment.

3.3.7 Sensible heat exchange at the skin surface

Q_t is the sum of Q_c and Q_r, and these are convective and radiative heat exchange rate between the skin surface and the environment described by equation 3.14 and 3.15 respectively.

$$Q_c = h_c\left(T_{sk,i} - T_a\right)A_i f_{cl}\left(1 - CSF_i\right) \tag{3.14}$$

$$Q_c = h_r \varepsilon \left(T_{sk,i} - T_a\right) A_i f_{cl} \frac{A_{r,i}}{A_{D,i}} (1 - CSF) \tag{3.15}$$

where CSF is the surface area rate in contact with external object, ε is the emissivity of the human skin, in the 33 NCM was used 0.95, but after some research, knows although closely similar to a perfect black body in his radiative properties, is equal to 0.98 [Delchar, 1997], A_r is the effective radiation area of the human body, A_D is the DuBois body surface area, both areas are described in table 3.5.

Table 3.5: Ratio A_r / A_D [Streblow, 2011]

Segment	sitting	standing
Head	1	1
Chest	0.7	0.7
Back	0.2	0.8
Pelvis	0.5	0.8
Shoulder	0.7	0.7
Arm	0.7	0.7
Hand	0.6	0.6
Thigh	0.7	0.8
Leg	1	0.8
Foot	0.75	0.75
All	0.7	0.77

3.3.8 Heat exchange by conduction with contacted surface

$Q_{mt,i}$ is the heat exchange by conduction in [W] between the skin layer and contacted surface described by equation 3.16.

$$Q_{mt,i} = \frac{CSF A_{sk,i} f_{cl} \left(T_{sk,i} - T_{mt,i}\right)}{0.155 I_{cl,i}} \tag{3.16}$$

3.4 Physiological active model

3.4.1 Sensor signals

The error signal $Err_{i,j}$ in [K] is calculated by equation 3.17. The set-point temperature $T_{set,i,j}$, which play a role to control the comfortable temperature, is shown in table 3.6.

$$Err_{i,j} = \left(T_{i,j} - T_{set,i,j}\right) \tag{3.17}$$

Table 3.6: Set-point temperature [Streblow, 2011]

Segment	Temperature [°C]	
	Core	Skin
Head	36.9	35.6
Chest	36.5	33.6
Back	36.5	33.2
Pelvis	36.3	33.4
Shoulder	35.8	33.4
Arm	35.5	34.6
Hand	35.4	35.2
Thigh	35.8	33.8
Leg	35.6	33.4
Foot	35.1	33.9

Warm signal $Wrm_{i,j}$ and cold signal $Cld_{i,j}$ both in [K], corresponding to warm and cold receptors, respectively, are defined by equation 3.18 (when $Err_{i,j} > 0$) and equation 3.19 (when $Err_{i,j} < 0$).

$$Wrm_{i,j} = Err_{i,j}, Cld_{i,j} = 0 \tag{3.18}$$

$$Cld_{i,j} = Err_{i,j}, Wrm_{i,j} = 0 \tag{3.19}$$

3.4.2 Integrated signal

The integrated sensor signals from skin thermoreceptores are used as the control variable. Integrated warm signal $Wrms$ and integrated cold signal $Clds$ both in [K] are defined by equations 3.20 and 3.21, respectively. The integrated sensor signals activate the mechanisms of the active system. $SKINR_i$ is the weighting coefficient for integration and is shown in table 3.7.

$$Wrms = \sum_{i=1}^{16} \left(SKINR_i Wrm_{i,sk} \right) \tag{3.20}$$

$$Clds = \sum_{i=1}^{16} \left(SKINR_i Cld_{i,sk} \right) \tag{3.21}$$

3.4.3 Thermoregulatory system of 33 NCM

All control equations consist of three terms. One is related with head core signal $Err_{1,1}$, another with skin signal $(Warms - Colds)$ and the last term is related with both $((Wrm_{1,1} * Wrms) or (Cld_{1,1} *$

Table 3.7: Weighting and distribution coefficients [Streblow, 2011]

Segment	SKINR	SKINS	SKINV	SKINC	Chilf
Head	0.070	0.081	0.320	0.022	0.020
Chest	0.149	0.146	0.098	0.065	0.258
Back	0.132	0.129	0.086	0.065	0.227
Pelvis	0.212	0.206	0.138	0.065	0.365
Shoulder	0.023	0.051	0.031	0.022	0.004
Arm	0.012	0.026	0.016	0.022	0.026
Hand	0.092	0.016	0.061	0.152	0.000
Thigh	0.050	0.073	0.092	0.022	0.023
Leg	0.025	0.036	0.023	0.022	0.012
Foot	0.017	0.018	0.050	0.152	0.000

$Clds$)). The thermoregulatory system consists of four control processes: vasodilation, vasoconstriction, perspiration, and shivering heat production. The distribution coefficient of individual segment for each control process is also shown in table 3.8. When the values for the four control processes calculated from the control equations become negative, they are set at 0.

Table 3.8: Control coefficients [Streblow, 2011]

	Core (C)	Skin (S)	Core X Skin (P)
Sweat (SW)	$C_{SW} = 371.2$	$S_{SW} = 33.6$	$P_{SW} = 0.0$
Shivering (Ch)	$C_{Ch} = 0.0$	$S_{Ch} = 0.0$	$P_{Ch} = 24.4$
Vasodilation (Dl)	$C_{Dl} = 117.0$	$S_{Dl} = 7.5$	$P_{Dl} = 0.0$
Vasoconstriction (St)	$C_{St} = 11.5$	$S_{St} = 11.5$	$P_{St} = 0.0$

3.4.4 Vasomotion

Skin blood flow $BF_{i,sk}$ in $[ls^{-1}]$ is calculated by equation 3.22. D_l and S_t are the signals for vasodilation (equation 3.23 in $[ls^{-1}]$) and vasoconstriction (equation 3.24), respectively.

$$BF_{i,sk} = \frac{BFB_{i,sk} + SKINV_i D_l}{1 + SKINC_i S_t} km_{i,sk} \tag{3.22}$$

$$D_l = C_{Dl} Err_{1,1} + S_{Dl}(Wrms - Clds) + P_{Dl} Wrm_{1,1} Wrms \tag{3.23}$$

$$S_t = -C_{St} Err_{1,1} + S_{St}(Wrms - Clds) + P_{St} Cld_{1,1} Wrms \tag{3.24}$$

In equations 3.22, $km_{i,sk}$ is called the "local multiplier", a factor for incorporating the effect of local skin temperature on vasomotion and perspiration, defined by equation 3.25. The local multiplier becomes:

$$km_{i,sk} = 2^{Err_{i,sk}/10} \tag{3.25}$$

3.4.5 Perspiration

The heat loss by evaporation of sweat $E_{sw,i,sk}$ is calculated by equation 3.26.

$$E_{sw,i,sk} = \left(C_{Sw}Err_{1,1} + S_{Sw}(Wrms - Clds) + P_{Sw}Wrm_{1,1}Wrms\right) SKINS_i km_{i,sk} \tag{3.26}$$

3.4.6 Shivering

The shivering heat production $C_{h,i,cr}$, is calculated by equation 3.27.

$$C_{h,i,cr} = \left(-C_{Ch}Err_{1,1} + S_{Ch}(Wrms - Clds) + P_{Ch}Cld_{1,1}Clds\right) Chilf_i \tag{3.27}$$

$Chilf_i$ is the distribution coefficient of the core layer of the shivering heat production as shown in table 3.7.

4 Proposed improvements to the model

4.1 Introduction

In this thesis, the focus is to improve malfunctions of the 33NCM by Streblow [2011]. In this chapter the calculation of the human body state is improved by new formulations for the heat balance, the heat production by external work and the evaporative heat loss on skin surface for each segment, was also improved the human physiology system. For the model evaluation simulation results for relevant variables are plotted against measurement data taken from the literature. Table 4.1 shown a resume of all the improvements made.

Table 4.1: List of improvements

Description	**Equation**		**Unit**
	Old	New	
Convective heat transfer coefficient, h_c	Table 3.2	4.1	$Wm^{-2}K^{-1}$
Radiative heat transfer coefficient, h_r	Table 3.2	4.9	$Wm^{-2}K^{-1}$
Clothing temperature, T_{clo}	Not existing	4.10	°C
Evaporative heat transfer coefficient, h_e	3.1	4.19	$Wm^{-2}K^{-1}$
Vapour permeation efficiency of clothing, i_{icl}	Constant=0.34	4.20	
Lewis ratio, LR	Constant=16.5	4.21	
Mean Skin Temperature, MST	Average(T_{sk})	4.32	°C
Core heat balance equation	3.2	4.33	
Skin heat balance equation	3.3	4.34	
Heat production by external work, W_{cr}	3.6	4.35	W

4.2 Structure

Besides all the improvements made, the structure of the program was changed, included the code, this due to code that was a little "primitive" and full of "if" conditions, and now the code have half of the code lines that had in the beginning. For the users are also much easier to use, the figure 4.1 and 4.2 it is a good example of that, It was adding a new box as shown in figure 4.3 to insert some simple parameters as the position of the person (Seated or standing), vapor permeation efficiency of clothing or the metabolic rate.

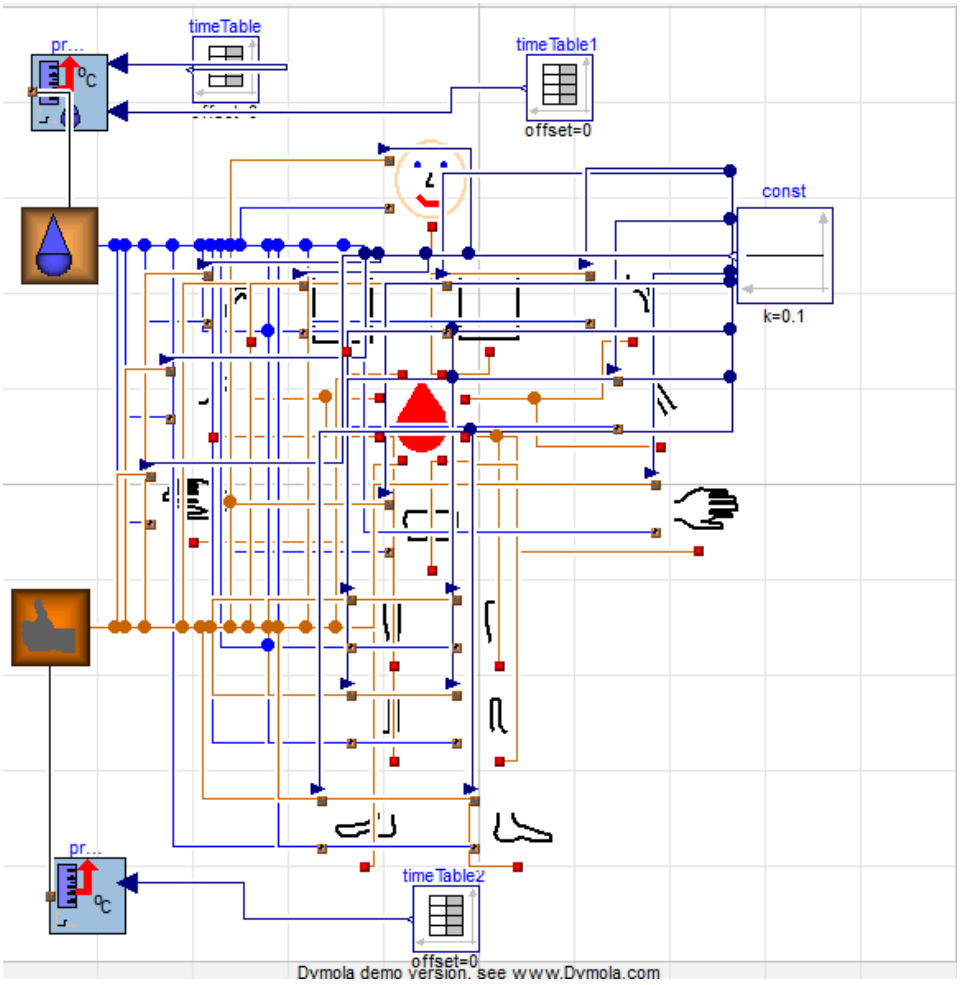

Figure 4.1: Old structure

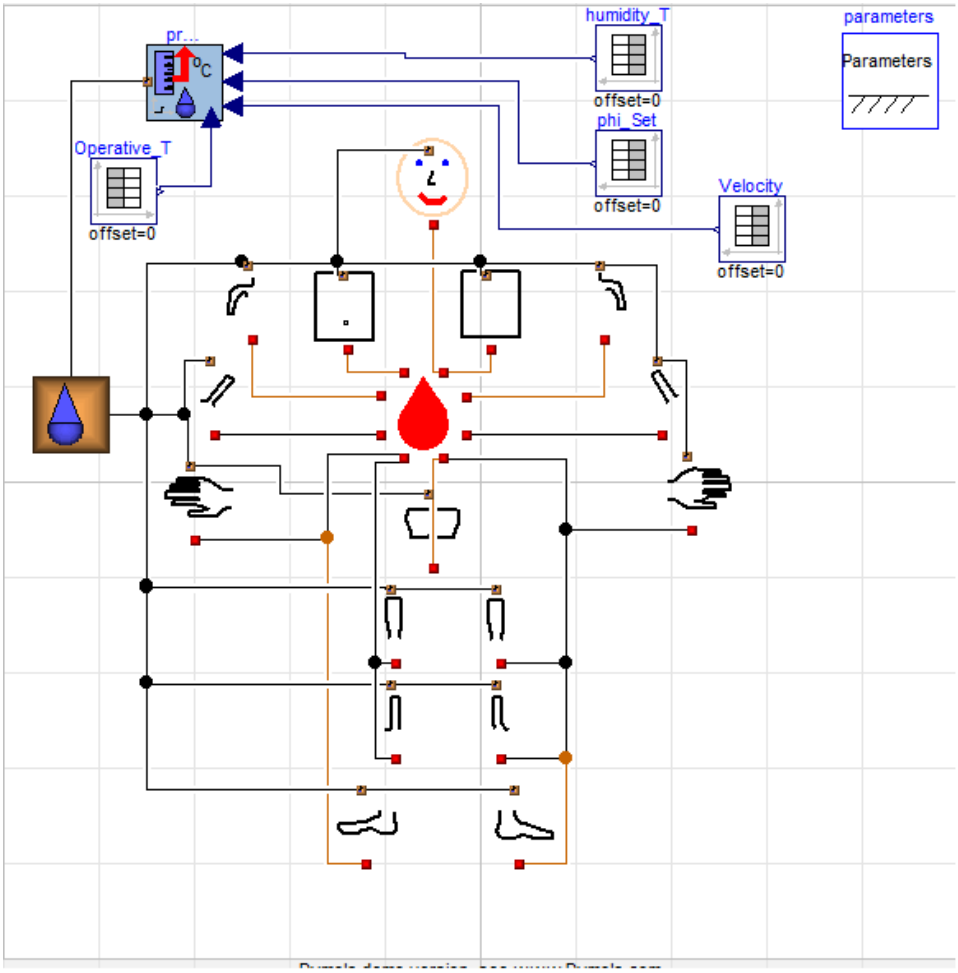

Figure 4.2: New structure

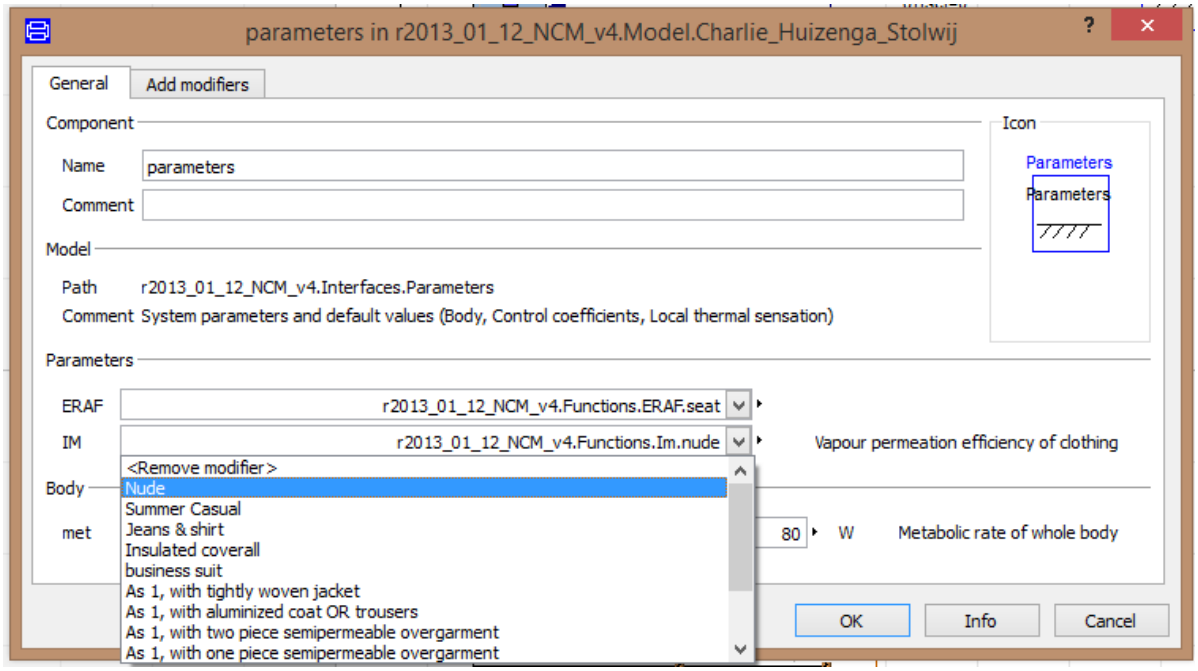

Figure 4.3: Parameters box

4.3 Human physiology

In this section is improved the convective, radiative and evaporative heat transfer coefficients. Instead of the obsolete constants used in convective and radiative heat transfer coefficients, now they are dependent on the environment. For the evaporative heat transfer coefficient, besides one error found the Lewis Ratio is now also dependent on the environment, instead of a constant.

4.3.1 Convection

In all three different convection modes explained in section 2.2.1, also the resistance of clothing has to be taken into account for the calculation of the heat transfer coefficient:

$$\frac{1}{h_c} = \begin{cases} \frac{1}{h_{c,n}} + 0.155 I_{cl} & , v \leq 0.2 \\ \frac{1}{h_{c,m}} + 0.155 I_{cl} & , 0.2 < v < 1.5 \\ \frac{1}{h_{c,f}} + 0.155 I_{cl} & , v \geq 1.5 \end{cases} \tag{4.1}$$

where h_c is the convective heat transfer coefficient in $[Wm^{-2}K^{-1}]$. $h_{c,n}$, $h_{c,m}$ and $h_{c,f}$ are natural (free), mixed and forced convective heat transfer coefficient, and calculated by equation 4.2, 4.3 and 4.8 respectively. The I_{cl} is the intrinsic clothing resistance in $[clo]$ and v is the air velocity in ms^{-1}.

The free convective heat transfer coefficient is calculated by Fanger equation [Fanger, 1970]:

$$h_{c,n} = 2.38\,(T_a - T_{sk})^{0.25} \tag{4.2}$$

where T_a and T_{sk} are the temperature of ambient and skin respectively in °C.

For the mixed convection the Nu can be used:

$$h_{c,m} = \frac{Nuk}{d} \tag{4.3}$$

where k is the thermal conductivity calculated in equation 4.24 and d is the characteristic dimension of the body or segment, given as the diameter of cylindrical segments $[m]$ and can be taken from the table. 4.2. de Dear calculated the Nusselt number Nu using the Reynolds number Re [de Dear et al., 1997]:

Table 4.2: Stolwijk's Characteristic radius [de Dear et al., 1997]

Segment	**Characteristic radius [m]**
Head	0.105
Trunk	0.142
Arms	0.044
Hands	0.015
Legs	0.064
Feet	0.016

$$Nu = CRe^b \tag{4.4}$$

$$Re = \frac{vd}{v} \tag{4.5}$$

where values C and b are 0.615 and 0.466 respectively in the range $400 < Re < 4000$, while in the range $4000 < Re < 40000$ correspond to 0.174 and 0.618 respectively. The v is the is kinematic viscosity $[m^2 s^{-1}]$, and is the ratio of the dynamic viscosity μ $[Pas]$ to the density of the fluid ρ $[kgm^{-3}]$:

$$v = \frac{\mu}{\rho} \tag{4.6}$$

where μ is computed using Sutherland's formula:

$$\mu = \mu_0 \left(\frac{0.555\tau_0 + SC}{0.555\tau + SC}\right)\left(\frac{\tau}{\tau_0}\right)^{\frac{3}{2}} \tag{4.7}$$

where initial dynamic viscosity μ_0 is 0.01827, τ is temperature in degrees Rankine [$^\circ R$] his initial temperature τ_0 is 524.07 and SC is Sutherland's constant, for standard air (120).

The forced convective heat transfer coefficient is calculated by de Dear equation [de Dear et al., 1997]:

$$h_{c,f} = K v^n \tag{4.8}$$

where K and n are constants and can be taken from the table. 4.3

Table 4.3: Dependence of convective heat transfer coefficient [de Dear et al., 1997]

Segment	sitting		standing	
	K	**n**	**K**	**n**
Head	4.90	0.730	3.20	0.970
Chest	9.10	0.590	7.50	0.660
Back	8.90	0.630	7.70	0.630
Pelvis	8.20	0.650	8.80	0.590
Shoulder	11.40	0.640	10.05	0.625
Arm	11.75	0.625	12.65	0.540
Hand	13.45	0.600	14.40	0.555
Thigh	8.90	0.600	10.10	0.520
Leg	13.15	0.580	12.85	0.505
Foot	12.90	0.545	12.00	0.495
All	10.10	0.610	10.40	0.560

4.3.2 Radiation

The radiative heat transfer coefficient h_r, besides being dependent on the environment, it can calculate for each body part from the expression [de Dear et al., 1997]:

$$h_{r,i} = 4\varepsilon\sigma \frac{A_{r,i}}{A_{D,i}} \left(273.15 + \frac{T_{cl,i} + T_a}{2}\right)^3 \tag{4.9}$$

where most of the constants are explained in section 3.3.7. σ is the Stefan-Boltzmann constant and T_{cl} is calculated by equation 4.10.

4.3.3 Heat and moisture transfer through clothing

The first purpose of clothing is protecting the human body against harmful environmental stresses. Thus, health, well being and productivity of humans depends on the clothing. Except the tropical

latitudes, humans normally use clothes every day, even at night when they are sleeping, humans need clothes to avoid freezing. Clothing influence strongly the physiological mechanisms. Clothes temperatures knowledge of the exact process, should not be underestimated, to reach the thermal comfort. The heat balance of the clothing node can be described as follows [Voelker et al., 2009]:

$$C_{p,cl}\frac{T_{cl}}{dt} = Q_{c,sk-cl} + Q_{e,sk-cl} - Q_{c,cl-a} - Q_{e,cl-a} - Q_{r,cl-a} + Q_{s,cl-a} \tag{4.10}$$

This heat balance contains the heat transfer from the skin to the clothing through conduction $Q_{c,sk-cl}$ and through evaporation $Q_{e,sk-cl}$. The heat exchange with the environment is described by the heat losses through convection $Q_{c,cl-a}$, evaporation $Q_{e,cl-a}$, radiation $Q_{r,cl-a}$ and possible gains due to solar radiation $Q_{s,cl-a}$. $C_{p,cl}$ indicates the heat capacity of the clothing, in these days the most common clothes material is cotton and polyester and the $C_{p,cl}$ varies from 750-1300 $\left[Jkg^{-1}K^{-1}\right]$.

4.3.3.1 Sensible heat transfer from skin to clothing node

The heat transfer from the skin node to the clothing node can be calculated using the equation 4.11 [Voelker et al., 2009].

$$Q_{c,sk-cl} = \frac{A_{cl,i}}{I_a I_{cl}}\left(T_{sk,i} - T_{cl,i}\right) \tag{4.11}$$

With I_a describes the insulation of the air layer, while I_{cl} is the effective insulation of the worn garments of the segment of the human body, average values can be seen in table 4.5.

4.3.3.2 Latent heat transfer from skin to clothing node

The amount of latent heat released from the skin is influenced by two issues. The first one it depends on the body's heat balance. Only in warm ambient conditions or high exercise levels will significant sweating occur. In the model, the evaporative heat transfer is firstly calculated as [Voelker et al., 2009]:

$$Q_{e,sk-cl,i} = \left(0.06 + 0.94\frac{Q_{e,sk-cl}}{E_{max,clo,i}}\right)E_{max,clo,i} \tag{4.12}$$

The second one, the environment's vapour pressure limits the ability of evaporation. The maximum evaporation of the human body is limited to the surrounding vapour pressure. $E_{max,clo,i}$ is used when assuming the skin being completely sweat covered and the partial vapour pressure of the air / clothing determines the maximum evaporative heat loss [Voelker et al., 2009].

$$E_{max,clo,i} = h_{e,clo,i} A_{clo,i} \left(p_{sk,i} - p_a\right) \tag{4.13}$$

The evaporative heat transfer coefficient $h_e[WPa^{-1}m^{-2}]$, a simplified equation is used for the calculation:

$$h_{e,clo,i} = \frac{LRi_{cl,i}}{0.155 I_{cl,i}} \tag{4.14}$$

where we use our own Lewis Ratio number calculated in equation 4.21 instead of the constant (16.5) as on the paper.

4.3.3.3 Sensible heat loss from clothing nto environment

The sensible heat exchange between the surface of the clothing and the environment are parted in 3 parts. The convective heat transfer, the long wave radiation exchange with the environment and the short wave absorption of solar radiation.

The convective term can be calculated as [Voelker et al., 2009]:

$$Q_{c,cl-a,i} = h_{c,clo,i} A_{clo} \left(T_{clo,i} - T_a\right) \tag{4.15}$$

Voelker [Voelker et al., 2009] used the table 4.4 to substitute the $h_{c,clo,i}$, but we just adjust the equation 4.1 and substitute all the $T_{sk,i}$ by $T_{clo,i}$.

Table 4.4: Convective heat transfer coefficients [Voelker et al., 2009]

Segment	h_c v=0.1ms^{-1}	$h_c = av^n$ v>0.1ms^{-1}	
		a	n
Head	3.7	11.75	0.625
Chest	3.0	9.10	0.590
Back	2.6	8.90	0.630
Pelvis	2.8	8.20	0.650
Shoulder	3.4	11.40	0.640
Arm	3.8	11.75	0.625
Hand	4.5	14.45	0.600
Thigh	3.7	8.90	0.600
Leg	4.0	13.15	0.570
Foot	4.2	12.90	0.545

The radiation heat exchange with the environment, Voelker based on Stefan-Boltzmann law.

$$Q_{r,cl-a,i} = f_{cl,i} A_{cl,i} \sigma \left(\varepsilon_{cl} \left(T_{cl,i} + 273.15 \right)^4 - \varepsilon_a \left(T_{a,i} + 273.15 \right)^4 \right) \tag{4.16}$$

The human body is not only exposed to the long-wave heat exchange with the environmental surfaces, but also to short-wave solar radiation. The incident radiation q_s on a specific oriented surface is calculated. The clothing node absorbs the short-wave radiation depending on the absorption coefficient of the clothing. In the model a value of $\alpha_{cl} = 0.6$ is considered [Voelker et al., 2009].

$$Q_{s,cl-a,i} = q_{s,i} A_{cl,i} \alpha_{cl} \tag{4.17}$$

4.3.3.4 Latent heat loss

The latent heat transfer from the clothing node to the environment can be calculated as.

$$Q_{e,cl-a,i} = h_{e,clo,i} A_{cl,i} \left(p_{cl,i} - p_a \right) \tag{4.18}$$

4.3.4 Evaporation

h_e is therefore an important means of evaporative heat transfer coefficient from the skin surface to the environment in certain circumstances, such as the cooling of the human body when it is subjected to ambient temperatures above the normal body temperature.

$$h_{e,i} = LR i_{cl,i} / \left(0.155 I_{cl,i} + \frac{i_{cl,i}}{h_{c,i} f_{cl,i}} \right) \tag{4.19}$$

4.3.4.1 Vapor permeation efficiency of clothing

The vapor permeation efficiency icl is an estimation using the description of the clothing type shown in table 4.5. The difference between cold and heat values represent the effect of condensation on the inner clothing surface, transforming evaporative to dry heat transfer [Havenith et al., 1999]. Intermediate values can be interpolated by equation 4.20.

$$i_{cl} = \frac{30 - T_a}{15} i_{cl,15} + \left(1 - \frac{30 - T_a}{15} \right) i_{cl,30} \tag{4.20}$$

Table 4.5: Example data for the estimation of the static clothing permeability index i_{cl} using description of the clothing type (data from [Havenith et al., 1999] and [Voelker et al., 2009]).

Clothing description	Estimated i_{cl} static **In the cold** <15°C	**In the heat** >30°C
Nude	0,50	
Men's summer casual	0,43	
Jeans & shirt	0,40	
Insulated coverall	0,39	
Men's business suit	0,37	
As 1, with tightly woven jacket	0,34	
As 1, with aluminized coat OR trousers	0,31	
As 1, with two piece semipermeable overgarment	0.17	0.15
As 1, with one piece semipermeable overgarment	0.14	0.13
As 1, with two piece impermeable overgarment	0.12	0.07
As 1, with one piece impermeable overgarment	0.10	0.06
As 1, with one piece impermeable overgarment, covered head except face, gloves, openings sealed (e.g., immersion suit)	0.06	0.02
Completely encapsulating suit, all openings sealed, no skin exposed	0.05	0.00

4.3.4.2 Lewis ratio number

In the 33 NCM model, the Lewis number LR is only a constant (16.5) as already mentioned, and we improved it with a formulation depended on temperature and ambient air pressure. So for the calculation of the LR we use the next equations (4.21)(4.22)(4.23) from Incropera [Incropera et al., 2011]:

$$LR = \frac{\alpha}{D_{AB}} \tag{4.21}$$

$$\alpha = \frac{k}{\rho C_{p,a}} \tag{4.22}$$

$$D_{AB} = \frac{T^{3/2}}{p_a} \tag{4.23}$$

where α is the thermal diffusivity, D_{AB} is the binary mass diffusivity, C_p is the heat capacity, p_a is the air pressure and T is the temperature of the air in °C. Also k changes with the temperature, when we use the equation (4.24) of Jacobson [Jacobson, 2005]. For equations (4.25) and (4.26) we use equation calculated by Morvay and Gvozdenac [Morvay and Gvozdenac, 2008].

$$k = k_d \left(1 - \left(1.17 - 1.02\frac{k_v}{k_d}\right) AH\right); \tag{4.24}$$

$$k_d = 2.43714 * 10^{-2} + 7.83035 * 10^{-5} T_a - 1.94021 * 10^{-8} T_a^2 + 2.85943 * 10^{-12} T_a^3 - 2.61420 * 10^{-14} T_a^4; \tag{4.25}$$

$$k_v = 1.74822 * 10^{-2} + 7.69127 * 10^{-5} T_v - 3.23464 * 10^{-7} T_v^2 + 2.59524 * 10^{-9} T_v^3 - 3.17650 * 10^{-12} T_v^4; \tag{4.26}$$

where k_d and k_v are the thermal conductivity of the dry air and saturated water vapor respectively, and AH is the absolute humidity, the relative humidity ϕ and temperature we can obtain using three equations, the equation for mixing ratio, an equation for relative humidity expressed in terms of mixing ratio and the Clausius-Claperyot equation, which relates the saturation vapor pressure to temperature. The result of combining the three equations is:

$$AH = \frac{1324\phi}{T + 273.15} exp\left[5417.15\left(\frac{1}{273} - \frac{1}{T + 273.15}\right)\right] \tag{4.27}$$

the relation holds true for $T > 0$, for $T < 0$ replace 5417,75 with 6139,81.

The heat capacity of the moist air C_p come from [Morvay and Gvozdenac, 2008] and is as follows:

$$C_p = C_{p,d} + AHC_{p,v} \tag{4.28}$$

$$C_{p,d} = 1.0029 + 5.4 * 10^{-5} T_d \tag{4.29}$$

$$C_{p,v} = 1.856 + 2 * 10^{-4} T_v \tag{4.30}$$

where $C_{p,d}$ and $C_{p,v}$ are the heat capacity of the dry air and saturated water vapor respectively. For the density of the moist air we use the equation of [Shelquist, 2012]:

$$\rho = \frac{p_d M_d + p_v M_v}{RT} \tag{4.31}$$

where M_d and M_v are the molar mass of the dry air and saturated water vapor respectively, and R is the universal gas constant.

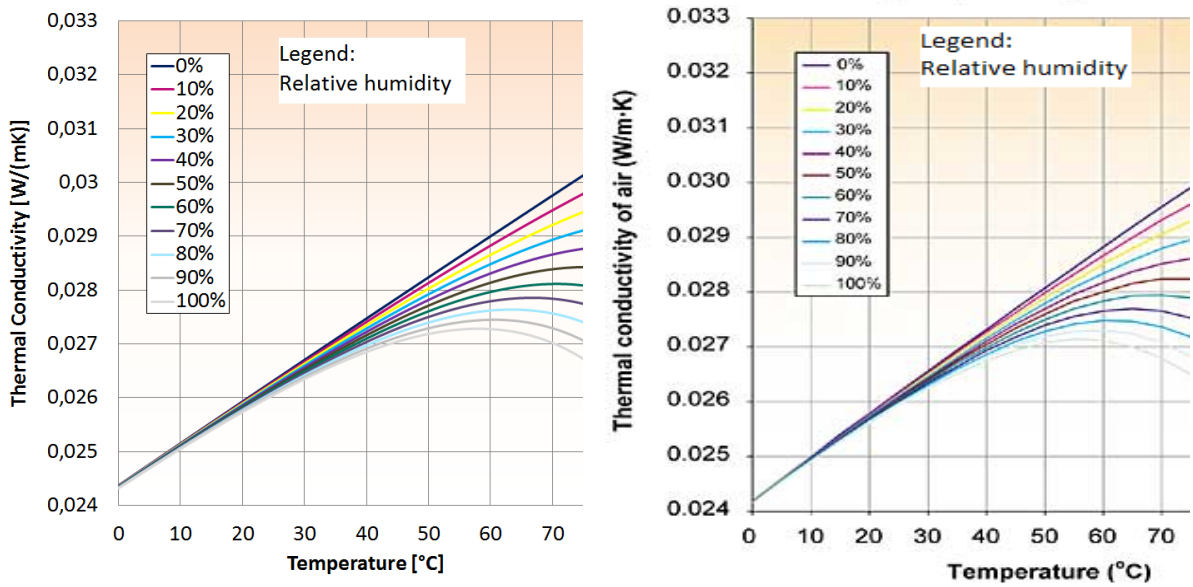

(a) Program simulation of thermal conductivity of moist air.

(b) Real measurements of thermal conductivity [Lasance, 2003]

Figure 4.4: Validation of the thermal conductivity

4.4 Mean Skin Temperature

From Hardy and DuBois [D.Hard and F.DuBois, 1938] we can easily understand that the Mean Skin Temperature (MST) in [°C] is calculated with a direct correlation from skin temperature times skin area, with the help of the table 4.6, we reach the new equation:

$$MST = \frac{\sum_{i=1}^{16} T_{sk,i} A_{sk,i}}{\sum_{i=1}^{16} A_{sk,i}} \tag{4.32}$$

4.5 Perspiration

During the research, it was found that the perspiration did not work correctly, after compared with different test cases from literature, concludes that the existing model showed a weak behaviour for perspiration. The errors were found, and based on data from literature the model is improved using new formulations for heat production by external work and evaporative heat transfer coefficient.

Table 4.6: Body surface area and body weight [Kobayashi and Tanabe, 2013]

i	$Segment$	$Area[m^2]$	$Wt[kg]$	$Wt_{cr}[kg]$	$Wt_{sk}[kg]$
1	Head	0.139	4.02	3.42	0.60
2	Chest	0.175	12.40	10.54	1.86
3	Back	0.161	11.03	9.38	1.65
4	Pelvis	0.221	17.57	14.93	2.64
5	Right Shoulder	0.096	2.16	1.84	0.32
6	Left Shoulder	0.096	2.16	1.84	0.32
7	Right Arm	0.063	1.37	1.16	0.21
8	Left Arm	0.063	1.37	1.16	0.21
9	Right Hand	0.050	0.34	0.29	0.05
10	Left Hand	0.050	0.34	0.29	0.05
11	Right Thigh	0.209	7.01	5.96	1.05
12	Left Thigh	0.209	7.01	5.96	1.05
13	Right Leg	0.112	3.34	2.84	0.50
14	Left Leg	0.112	3.34	2.84	0.50
15	Right Foot	0.056	0.48	0.41	0.07
16	Left Foot	0.056	0.48	0.41	0.07
	Total	1.868	74.43	63.27	11.17

4.5.1 Heat Balance

The heat capacity [$Whkg^{-1}°C^{-1}$] values are taken from table 4.7, and the weight was not being on account. Where the heat balance equations for core and skin are calculated by equation 4.33 and 4.34 respectively.

$$C_{p,cr,i} Wt_{cr} \frac{dT_{cr,i}}{dt} = Q_{cr,i} + B_{cr,i} - D_{cr,i} - RES_{cr,i} \tag{4.33}$$

$$C_{p,sk,i} Wt_{sk} \frac{dT_{sk,i}}{dt} = Q_{sk,i} + B_{sk,i} - D_{sk,i} - Q_{t,sk,i} - E_{sk,i} \tag{4.34}$$

where Q is the rate of heat production, B is the heat exchange rate between central blood compartment and each node, D is the conductive heat exchange rate with neighbouring layer, RES is the heat loss by respiration, W_t is the weight, Q_t is the convective and radiant exchange rate between skin surface and the environment and E is the evaporative heat loss at the skin surface. The skin weight for each body part is 15% of the weight showed in table 4.6 [Farabee, 2010].

Table 4.7: Heat capacity [$Whkg^{-1}°C^{-1}$][Kobayashi and Tanabe, 2013]

Segment	Core layer	Skin layer
Head	1.7229	0.189
Chest	10.2975	0.441
Back	9.3935	0.406
Pelvis	13.8340	0.556
Shoulder	1.6994	0.126
Arm	0.1209	0.084
Hand	0.1536	0.088
Thigh	5.3117	0.334
Leg	2.8670	0.169
Foot	0.2097	0.107
Central blood compartment		1.999

4.5.2 Heat production by external work

External work can be considered in terms of the activity of muscle cells (core layer) in the body. Unlike the equation 3.6 the heat production of external work W_{cr} that had a small mistake and now corrected and shown as:

$$W_{cr,i} = (met - Q_{b,i})AMetf_i \tag{4.35}$$

where met this time is the metabolic rate in [W].

4.5.3 Evaporative heat loss at skin surface

The evaporative heat loss E, is expressed by eq. 4.36. It consists of water vapor diffusion through the skin E_b defined by eq. 4.37 and the evaporation of insensible sweat E_{sw} depending on a few control and distribution coefficients plus set-point temperatures all described more in detail in the physiological active model in [Streblow, 2011]. The skin diffusion is assumed to be 6% of the maximum evaporative heat loss E_{max} eq. 4.38.

$$E_{sk,i} = E_{b,i} + E_{sw,i} \tag{4.36}$$

$$E_{b,i} = 0.06\left(1 - \frac{E_{sw,i}}{E_{max,i}}\right)E_{max,i} \tag{4.37}$$

$$E_{max,i} = h_{e,i} \left(p_{sk,i} - p_a \right) A_i \tag{4.38}$$

where h_e is the evaporative heat transfer coefficient from the skin surface to the environment and given in more detail in section 4.3.4.

In this case the equations are the same, but with the improved evaporative heat transfer coefficient h_e, now make all the difference, as can bee seen in figure 4.5.

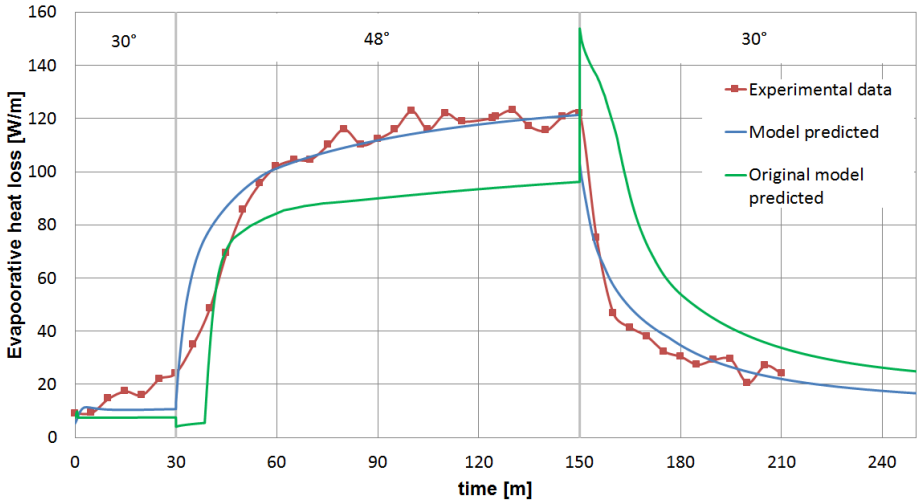

Figure 4.5: Comparison between measurements and simulated data of the evaporative heat loss during hot step-change conditions from 30°C, 40% RH to 48°C, 30% RH, from [Huizenga et al., 2001]

5 Results and sensitivity

This chapter serves for the purpose of testing and validating all the improvements. For validation of the 33 NCM different data from literature are used. It begins with the pure passive system, where a dead man's case is tested, followed by the validation of the thermal neutrality and by a deeper analysis of the active system. All these test cases are described in the next sections.

5.1 Passive system

In this case we switched off all the active system control mechanisms (sweating, shivering and vasomotion). The literature tests a dead man, what is perfect for this situation. We compare only the rectal temperature. The system and boundary conditions are shown in table 5.1.

Table 5.1: System and boundary conditions:
dead man in a cold environment

Quantity	Value	Unit	Description
T_{in}	37	°C	Initial temperature of the chest
T_a	10	°C	Ambient temperature
v_a	0.1	ms^{-1}	Environment air speed
ϕ	30	%	Environment air relative humidity
Position			Sedentary

The comparison of simulated rectal temperature with results presented in literature [THESEUS-FE, 2012] is shown in figure 5.1. In the dead body case, only heat conduction from the core to the skin, and convection and radiation from the skin to the environment exist.

5.2 Thermal neutrality

These two cases serve to evaluate the 33 NCM model in a thermal neutrality case. Where the test cases expose the humans in a thermal comfortable environment.

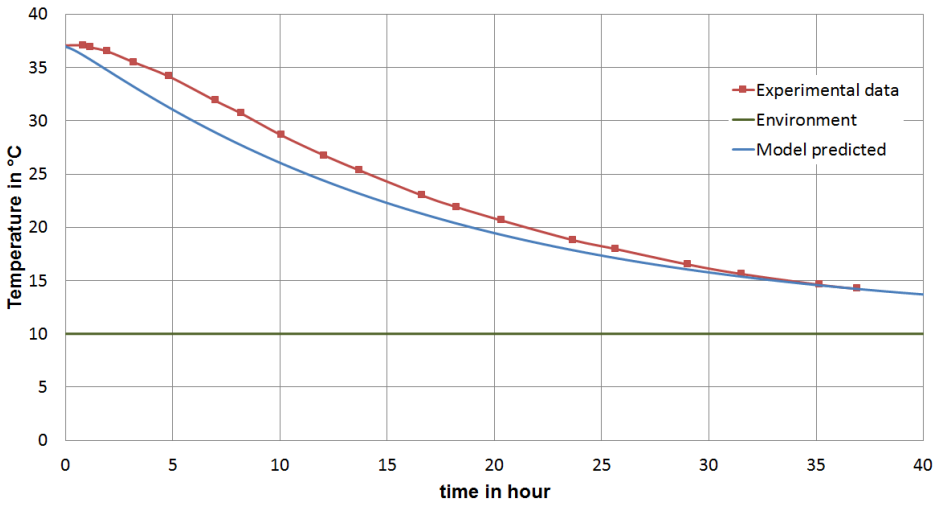

Figure 5.1: Dead man, rectal temperature

5.2.1 Thermal neutrality in naked person

In the case of thermal neutrality the environmental temperature is changed to 30 °C, which gives a comfortable environment for a naked person. When the human body is in a comfortable equilibrium the metabolic mechanisms like perspiration, vasomotion or shivering are in a low heat production state. In this situation, we only compare the 33 NCM model with THESEUS-FE model and Fiala PhD thesis. The system and boundary conditions are shown in table 5.2.

Table 5.2: System and boundary conditions:
constant temperature for a naked person

Quantity	Value	Unit	Description
met	83	W	Metabolic activity
T_a	30	°C	Ambient temperature
v_a	0.05	ms^{-1}	Environmental air speed
ϕ	40	%	Environmental air relative humidity
Position			Standing

The comparison shown in table 5.3 concludes that the 3 different models are very similar. It should be noted that the mean convective heat transfer coefficient $h_{c,mn}$ in the 33 NCM is higher than the other models, and the skin heat loss Q_{sk} is 10 W lower than the others.

Table 5.3: Comparison between Fiala [Fiala, 1998], THESEUS-FE [THESEUS-FE, 2012] and 33 NCM [Streblow, 2011] models

Quantity	Fiala	THESEUS-FE	33 NCM	unit	Description
W_t	73.50	73.53	74.43	kg	Body weight
A_{sk}	1.90	1.86	1.87	m^2	Skin surface area
Q_b	87.10	87.13	84.62	W	Basal metabolic rate
MST	34.40	34.43	34.72	°C	Mean Skin Temperature
$T_{cr,h}$	37.00	36.90	37.01	°C	Head core temperature
$T_{cr,ab}$	36.88	36.80	36.77	°C	Abdomen core temperature
$h_{c,mn}$	2.70	2.66	3.41	$Wm^{-2}K^{-1}$	Mean convective heat transfer coefficient
$h_{r,mn}$	5.00	4.50	4.27	$Wm^{-2}K^{-1}$	Mean radiative heat transfer coefficient
Q_{sk}	78.50	78.17	68.64	W	Skin heat loss
Q_{con}	21.50	21.89	23.15	W	Heat loss by convection
Q_r	38.90	37.02	31.05	W	Heat loss by radiation
Q_e	18.10	19.26	14.44	W	Heat loss by evaporation
Q_{rsp}	8.50	8.96	11.87	W	Heat loss by respiration
Q_{sum}	87.00	87.13	80.51	W	Sum of heat losses

5.2.2 Thermal neutrality for clothed person

Compared with section 5.2.1 we change the environmental temperature and the clothing and activity level of the person as shown in table 5.4. In this case the data from the literature include measurements for single body parts from experiments with 32 different persons [Fiala, 1998].

Table 5.4: System and boundary conditions: constant temperature for clothed person

Quantity	Value	Unit	Description
met	104	W	Metabolic activity
T_a	25.5	°C	Ambient temperature
$T_{r,mn}$	25.5	°C	Mean radiant temperature
v_a	0.10	ms^{-1}	Environmental air speed
ϕ	40	%	Environmental air relative humidity
I_{cl}	0.60	clo	Intrinsic clothing resistance
Position			Sedentary

As the table 5.5 and figure 5.2 show, the result of the 33 NCM model is pretty close to the measurements. But the calculation of the foot temperature is still not perfect, due to the diameter used in the calculation.

Table 5.5: Comparison between skin temperature distribution for resting man in comfort according to Fiala [1998] and 33 NCM

Segment	experiment	33NCM	unit
Rectal	36.9	36.2	°C
Head	34.2	34.2	°C
Chest	34.5	34.4	°C
Arm	32.1	33.0	°C
Hand	33.5	34.7	°C
Leg	32.9	31.8	°C
Foot	32.3	34.8	°C
Mean skin	32.5	33.4	°C

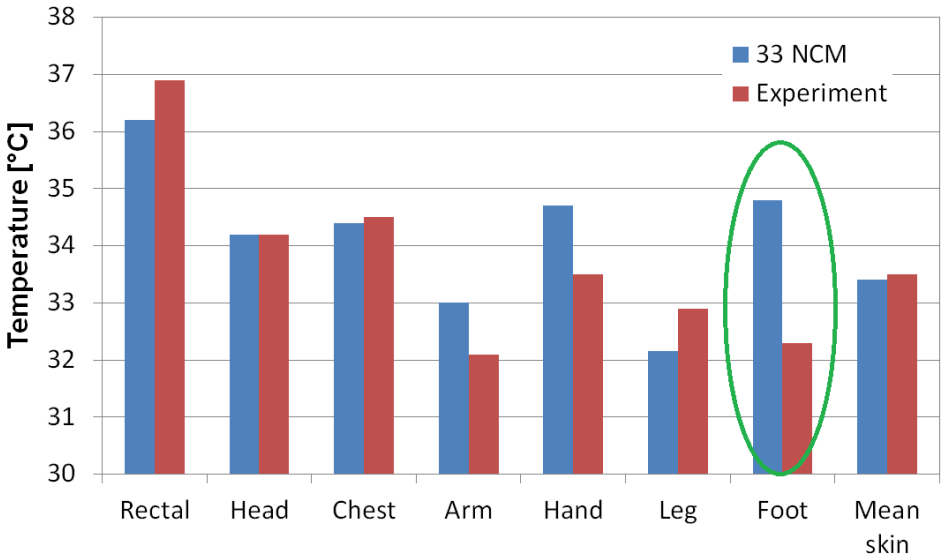

Figure 5.2: Comparison between skin temperature distribution for resting man in comfort according to Fiala [1998] and 33 NCM

5.3 Active system

The activity of the active system with sweating or shivering and vasomotion is proportional to the deviation from a comfortable state. So in this section more extreme situations are evaluated. The most important evaluation is when simulated at higher temperature, for it validates the perspiration process.

5.3.1 Cooling at 5°C

In this cooling case, the body is exposed to an extreme cold environment. Before the experiment the person stands 20 min at 24 °C[THESEUS-FE, 2012]. The preconditioning phase is not shown in the figures 5.3, 5.4 and 5.5. The system and boundary conditions are shown in table 5.6.

Table 5.6: System and boundary conditions:
cooling at 5°C

Quantity	Value	Unit	Description
met	83	W	Metabolic activity
T_a	5	°C	Ambient temperature
$T_{r,mn}$	5	°C	Mean radiant temperature
v_a	0.10	ms^{-1}	Environmental air speed
ϕ	30	%	Environmental air relative humidity
I_{cl}	0.10	clo	Intrinsic clothing resistance
Position			Standing

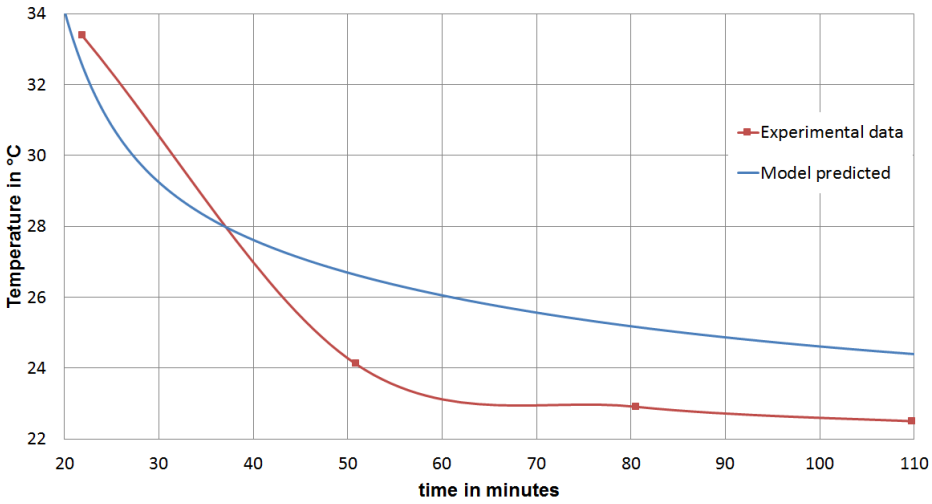

Figure 5.3: Cold environment, Mean Skin Temperature

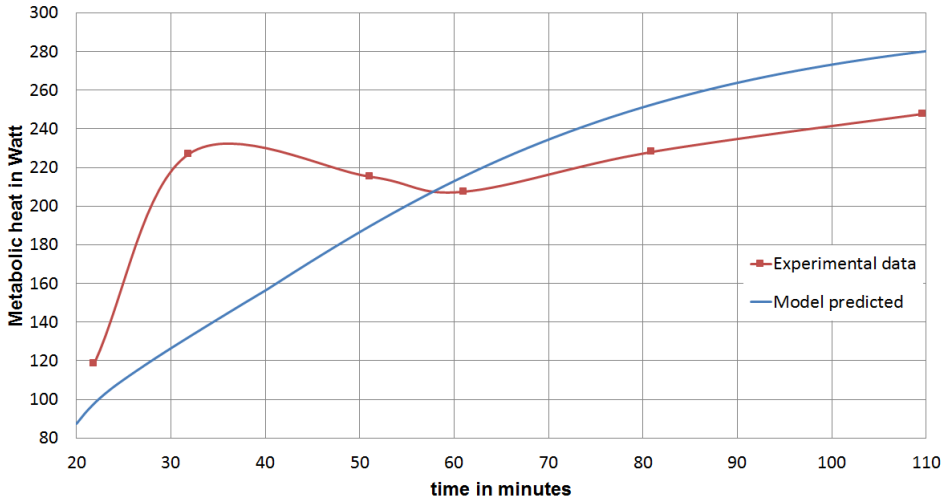

Figure 5.4: Cold environment, metabolism

As shown in figure 5.5, the rectal temperature does not fit to the measurements from THESEUS-FE [2012]. When the 33 NCM model is simulated in the cooling process, the curve falls down, unlike the experimental data. During the validation phase, this problem was found. It always occurs in cooling environment conditions, in other words, over estimate of shivering. The base equation of shivering is dependent on the head core temperature. This might be the problem, as shown in figure 5.4 the metabolism in the experimental data has a fast increase, and decrease afterhalf hour, and returns to rise again. When 33 NCM simulated at extreme cool condition, the head core temperature will always be decreased. Possibly the shivering equation is not correct.

This means the program needs some further improvements in the shivering process, as the metabolic heat and the temperature are unpredicted. But the overall behaviour shows the correct tendency.

5.3.2 Cooling at 5°C(2)

In this case the first 25 min the temperature is 28 °C, and 45% relative humidity. Afterwards the temperature decreases until 5°C, and the biggest difference in this case compared with section 5.3.1 is the relative humidity increases until 70% at 30 min. The system and boundary conditions are shown in table 5.7.

As can be seen in figure 5.6, 5.9 and 5.10, the simulation is pretty close from reality. But, in figure 5.7, 5.11 and 5.12, the results are different from measurements. Once again in this situation, when in a very cool environment the program has some fails as already explained in section 5.3.1.

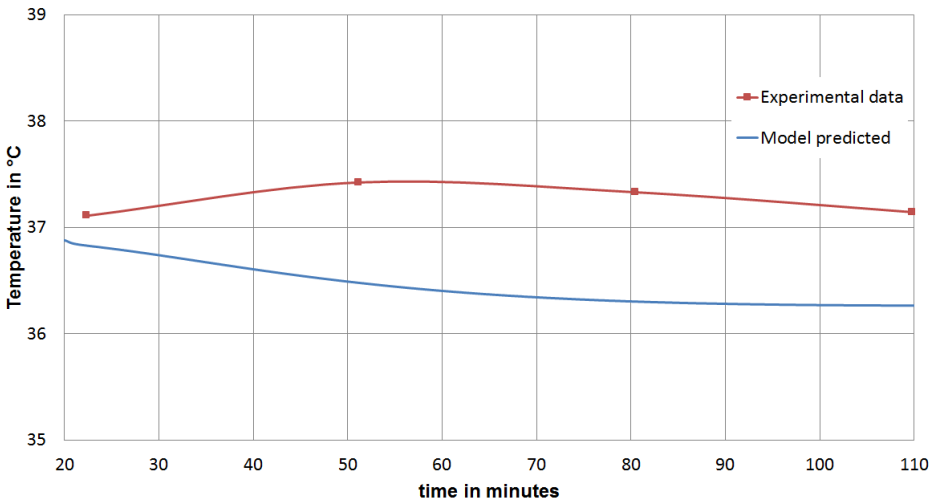

Figure 5.5: Cold environment, rectal temperature

Table 5.7: System and boundary conditions:
cooling at 5°C

Quantity	Value	Unit	Description
met	83	W	Metabolic activity
v_a	0.10	ms^{-1}	Environment air speed
I_{cl}	0.10	clo	Intrinsic clothing resistance
Position			Standing

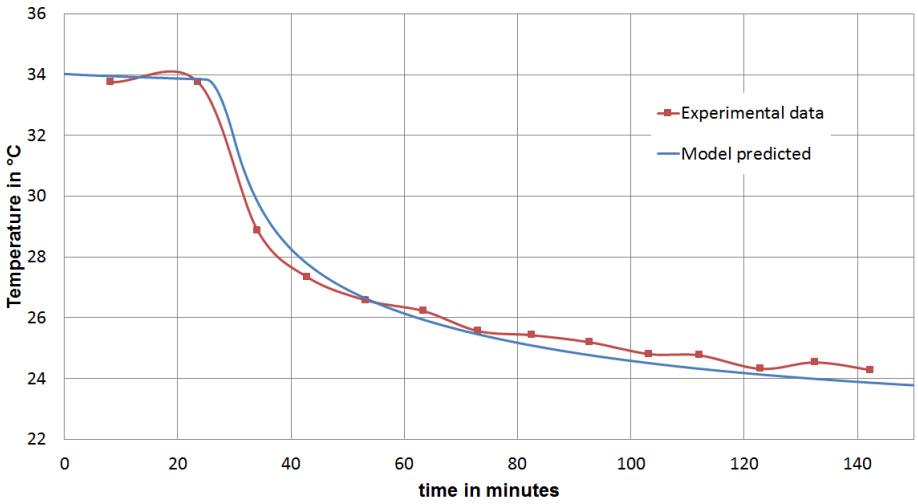

Figure 5.6: Cold environment (2), Mean Skin Temperature

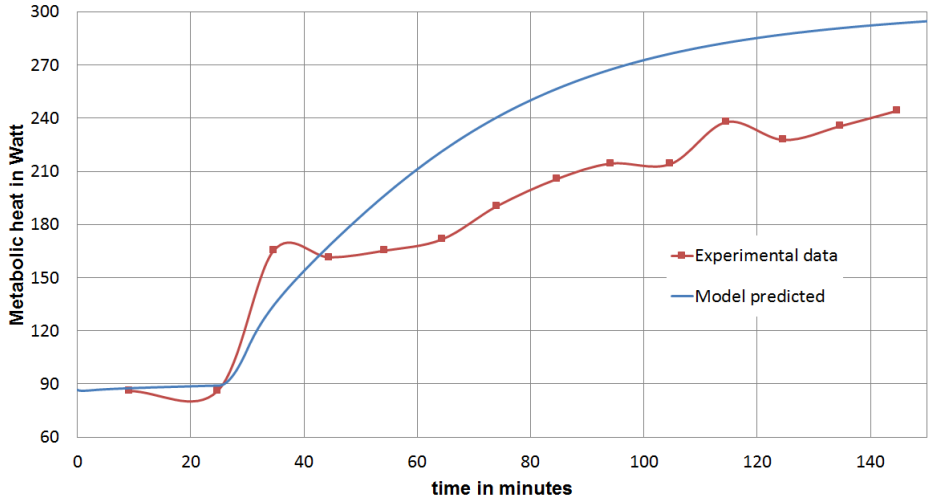

Figure 5.7: Cold environment (2), metabolism

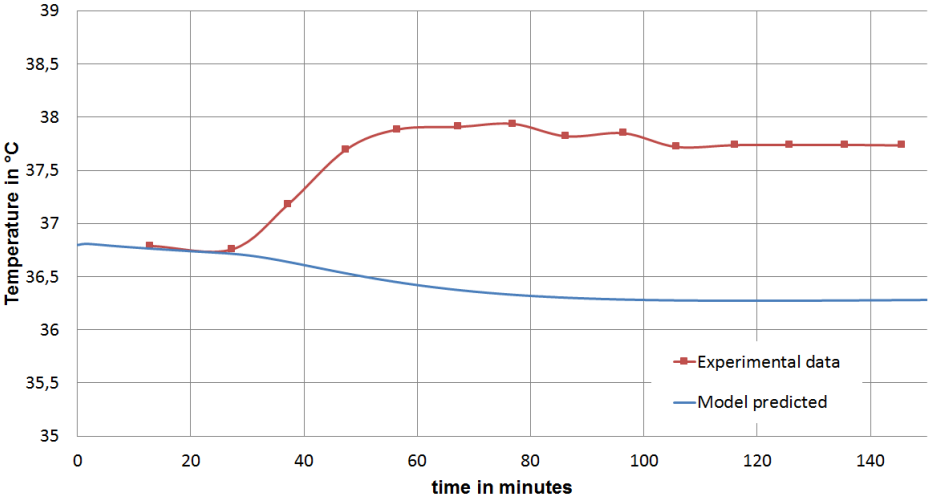

Figure 5.8: Cold environment (2), rectal temperature

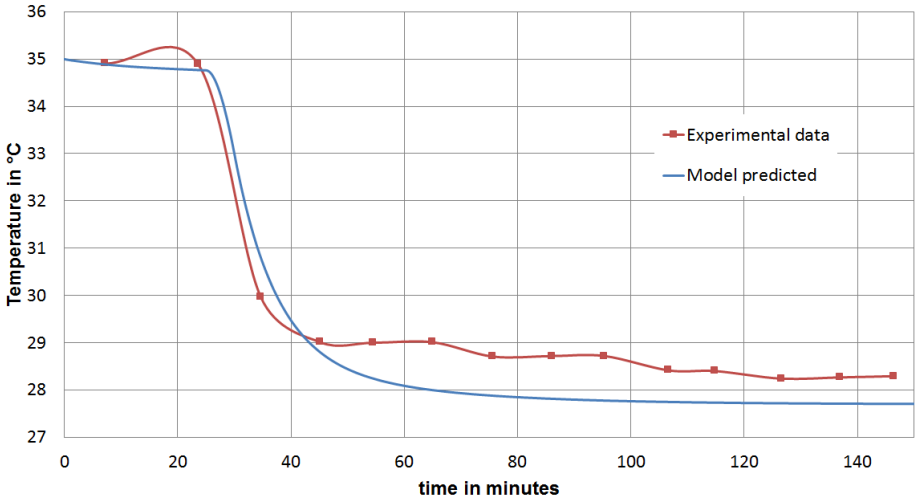

Figure 5.9: Cold environment (2), head temperature

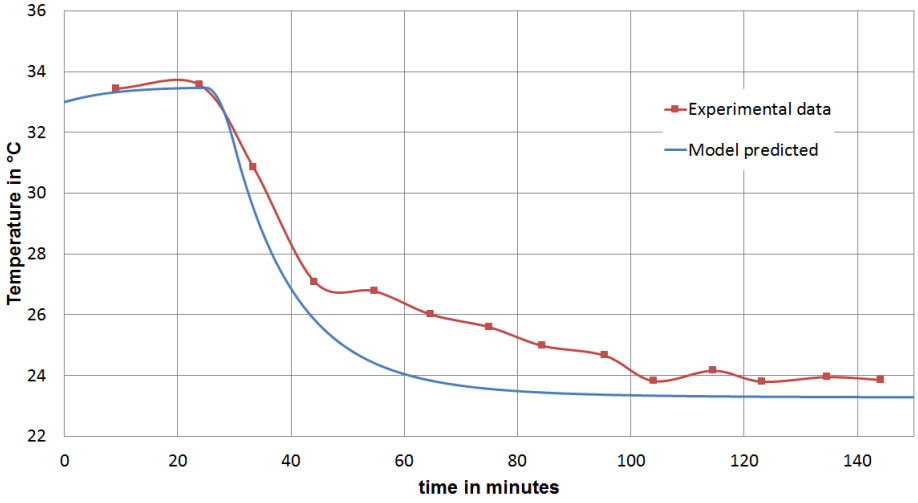

Figure 5.10: Cold environment (2), leg temperature

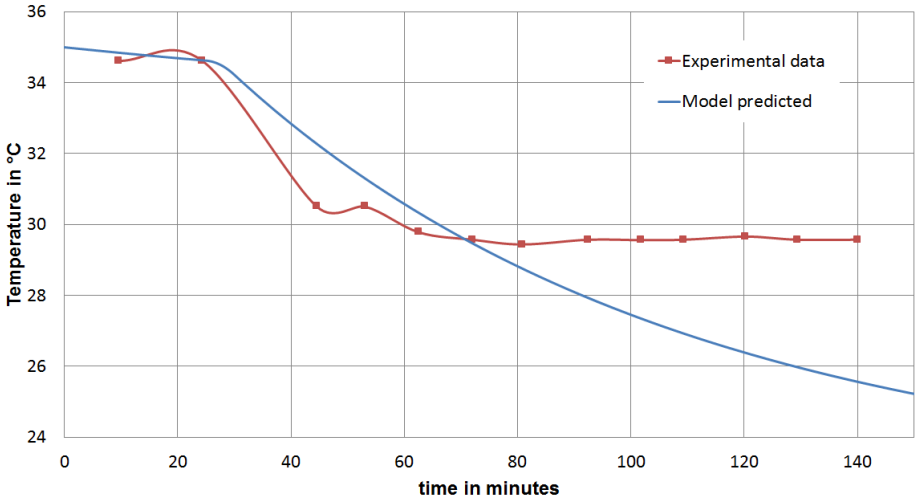

Figure 5.11: Cold environment (2), chest temperature

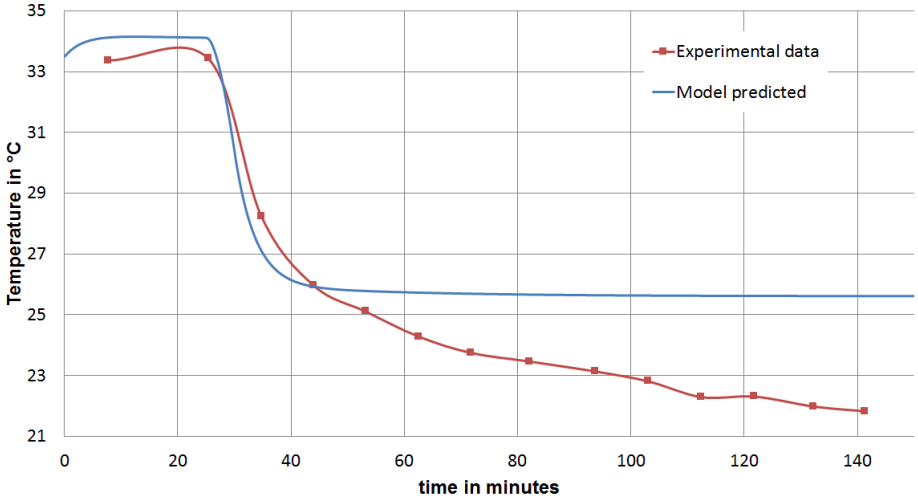

Figure 5.12: Cold environment (2), arm temperature

5.3.3 Changing environment 29-22-29°C

In this case during 60 min the temperature is 28 °C, with a 44% relative humidity, followed by a 120 min exposure period at 22 °C, and 39% relative humidity, and finally 60 min more with an exposure at 28 °C, and 41% relative humidity, as shown in figure 5.13. During the measurements the men walked rapidly from one climatic chamber to the next, in order to prevent the subject from having any loss of data during the 5 min period of the transient change [Hardy and Stolwijk, 1966]. The system and boundary conditions are shown in table 5.8.

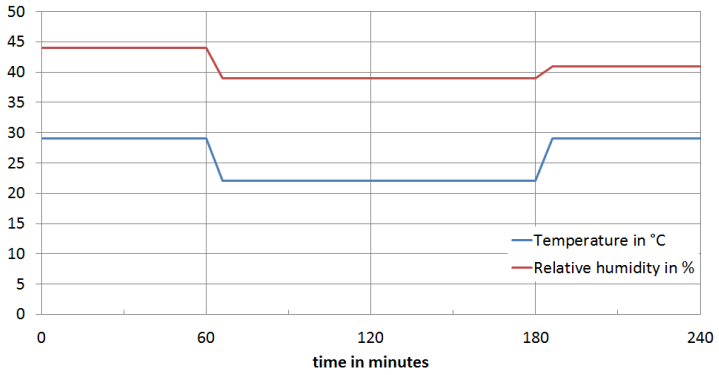

Figure 5.13: Boundary temperatures and relative humidity

Table 5.8: System and boundary conditions:
changing environment 29-22-29°C

Quantity	Value	Unit	Description
met	83	W	Metabolic activity
v_a	0.10	ms^{-1}	Environment air speed
I_{cl}	0.10	clo	Intrinsic clothing resistance
Position			Seated

As can be seen from the validation cases the model behaviour seems to be correct at higher temperatures but in colder environments has some flaws. The metabolism shows a stronger deviation compared to measurements, as shown in figure 5.15. In measurements the metabolism is almost stable whereas for the simulations with the 33 NCM the metabolism begins to rise in the cold chamber, and this change the mean skin temperature as can be seen in figure 5.17, but still even with the bad correlation at minute 180, the tendency is still right. As shown in figure 5.14, the 33 NCM has an almost stable evaporative heat loss around 5 Wm^{-2}. The measured higher values at the beginning of the experiment cannot be explained as no precondition data exist. At minute 180, there is a little high pic, which is due to the walking to the next chamber.

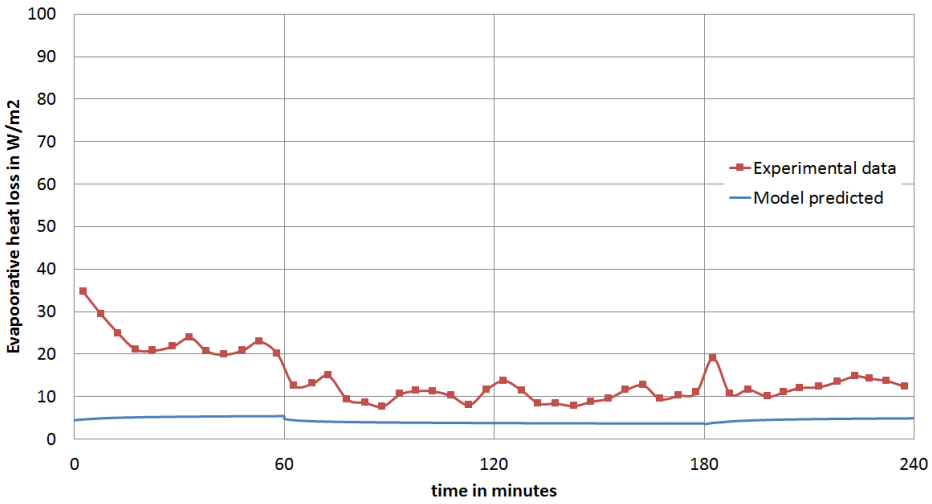

Figure 5.14: Changing environment 29-22-29°C, evaporative heat loss

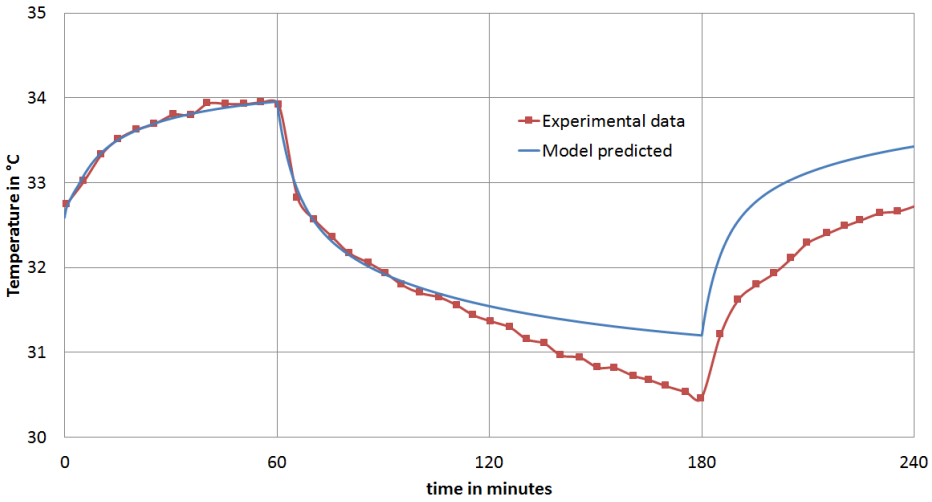

Figure 5.15: Changing environment 29-22-29°C, Mean Skin Temperature

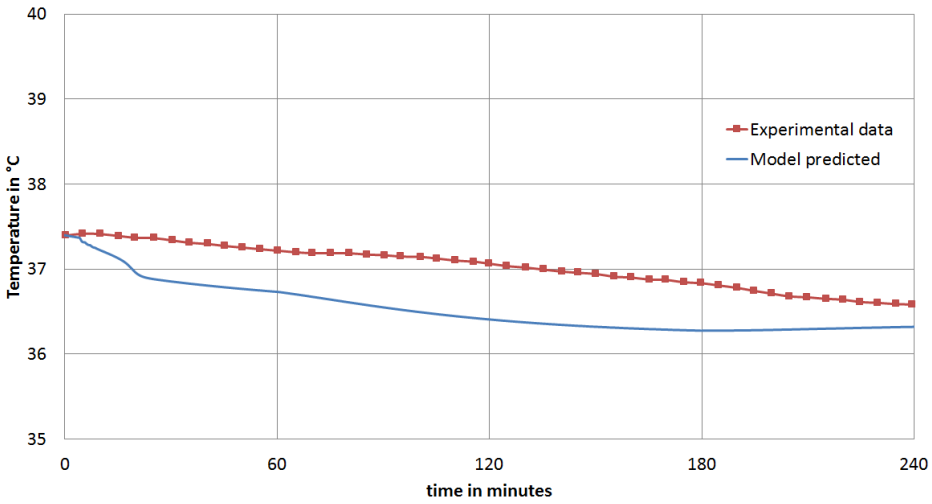

Figure 5.16: Changing environment 29-22-29°C, rectal temperature

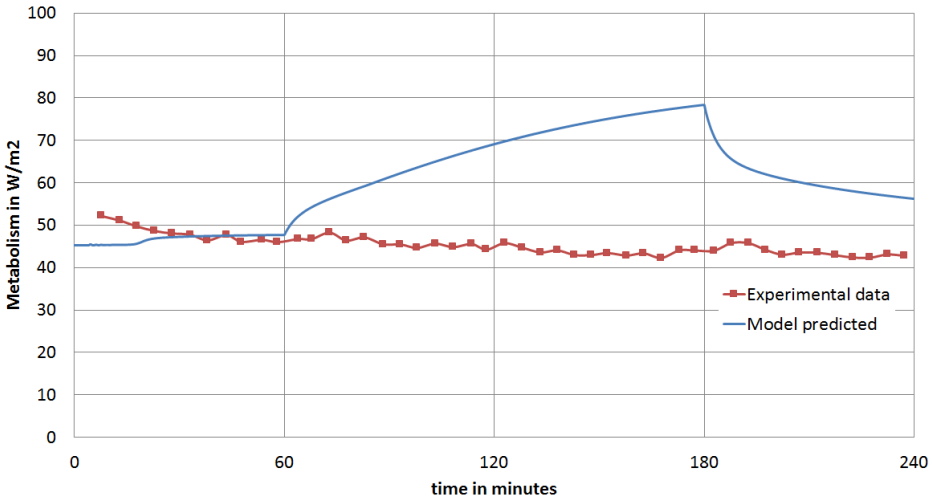

Figure 5.17: Changing environment 29-22-29°C, metabolism

5.3.4 Changing environment 30-48-30°C

In this case, during 30 min the temperature is 30 °C, with a 40% relative humidity, followed by 120 min exposure at 48 °C, and 30% relative humidity, and finally 60 min more with an exposure at 30 °C, and 40% relative humidity, as shown in figure 5.18 [Huizenga et al., 2001]. In this case there are several missing data. Table 5.9 was all presumed.

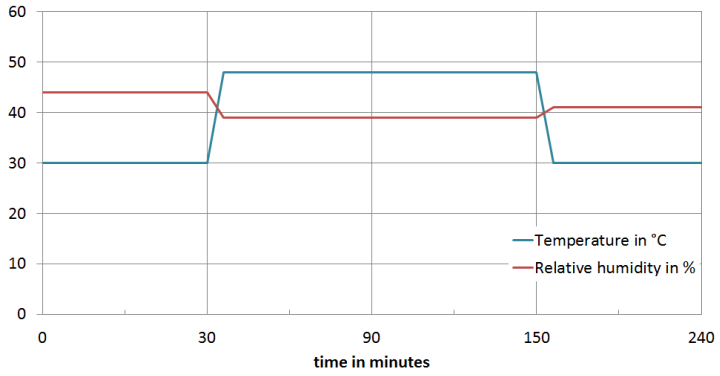

Figure 5.18: Boundary temperatures and relative humidity

Table 5.9: System and boundary conditions: changing environment 30-48-30°C

Quantity	Value	Unit	Description
met	83	W	Metabolic activity
v_a	0.10	ms^{-1}	Environment air speed
I_{cl}	0.10	clo	Intrinsic clothing resistance
Position			Seated

Figure 5.19 shows a good correlation between simulated data and measurements for the evaporative heat loss. Also the mean skin temperature is well predicted under very high temperatures. But for the low temperature of 30 °C the 33 NCM calculates a mean skin temperature which is about 1 K higher. The measured rectal temperature decreases over the whole experimental period (figure 5.21), but the 33 NCM predicts a changing temperature characteristic.

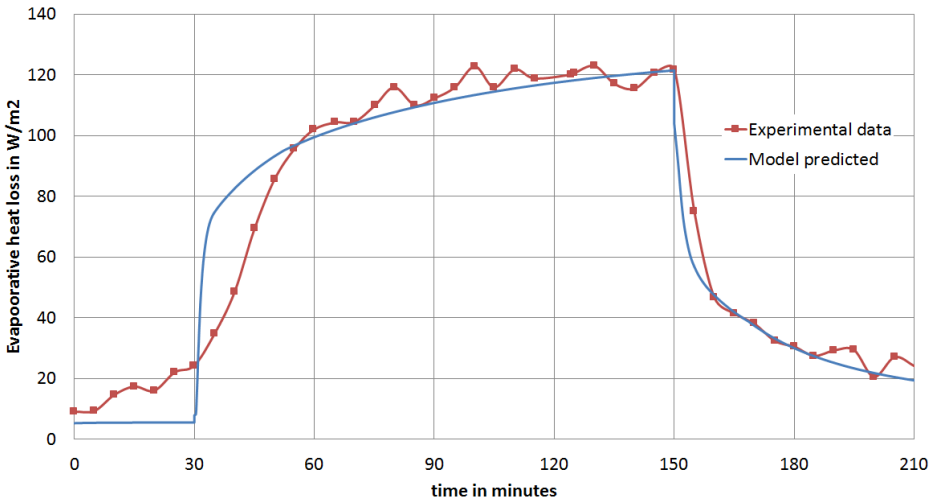

Figure 5.19: Changing environment 30-48-30°C, evaporative heat loss

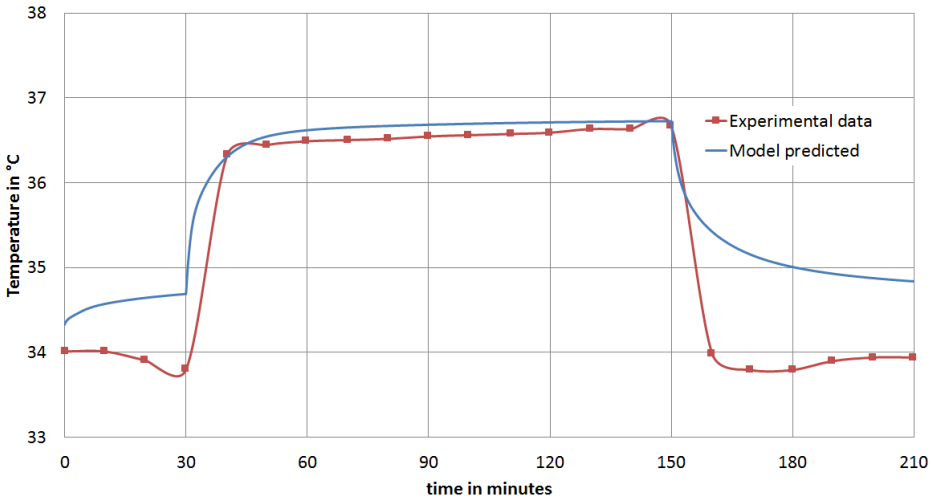

Figure 5.20: Changing environment 30-48-30°C, Mean Skin Temperature

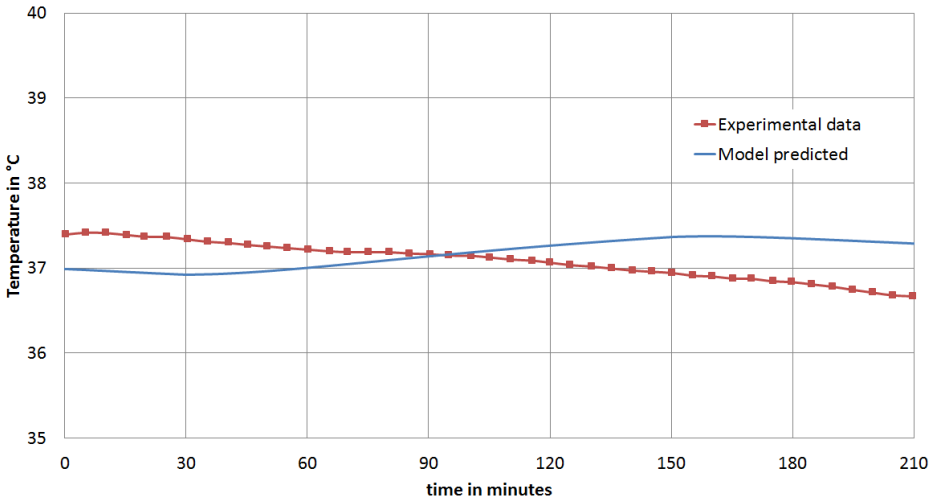

Figure 5.21: Changing environment 30-48-30°C, rectal temperature

6 Coupled Simulation

6.1 Introduction

CFD, an abbreviation of Computational Fluid Dynamic, is a branch of fluid mechanics that uses algorithms and numerical methods to analyze and solve problems that involve fluid flows. With the help of computers, it can perform calculations to simulate the interactions of gases and liquids with surfaces defined by boundary conditions. Sometimes high-speed supercomputer is needed to archive faster and better solution.

6.2 Model predicted in CFD

Besides the usage as a stand-alone tool, as shown in the last chapters, the 33 NCM can be also used in a coupled mode with numerical flow simulations (CFD). In this case the body surface temperature calculated within the 33 NCM is transferred to the CFD solver. The CFD domain includes a virtual manikin which is separated into the 16 body segments of the 33 NCM. Within the CFD calculation the flow distribution and the thermal boundary conditions of the manikin are calculated. From the flow field the radiative and convective heat transfer coefficients are extracted and transferred back to the 33 NCM. With those boundary conditions the 33 NCM calculates a new human body state resulting in a new surface temperature which goes back to the CFD calculation. Furthermore the thermal sensation and comfort voting are transferred to the CFD calculation for post-processing. In this thesis, the 33NCM is coupled with CFD using the commercial flow solver ANSYS Fluent 14.5. As co-simulation environment the TISC server from TLK Thermo is used. The TISC server synchronizes the subsimulations.

6.3 Experimental case

With a test case in compliance with Fanger's [Ostergaard et al., 1974] test case the stability of the model in a coupled mode is analyzed. A subject is exposed to a uniform velocity from in front as shown in fig. 6.1. The air is supplied over an rectangular area of 1.16 m^2 in a distance of 0.3 m to the subject. The supply velocity is 0.8 ms^{-1} with a temperature of 27.3 °C.

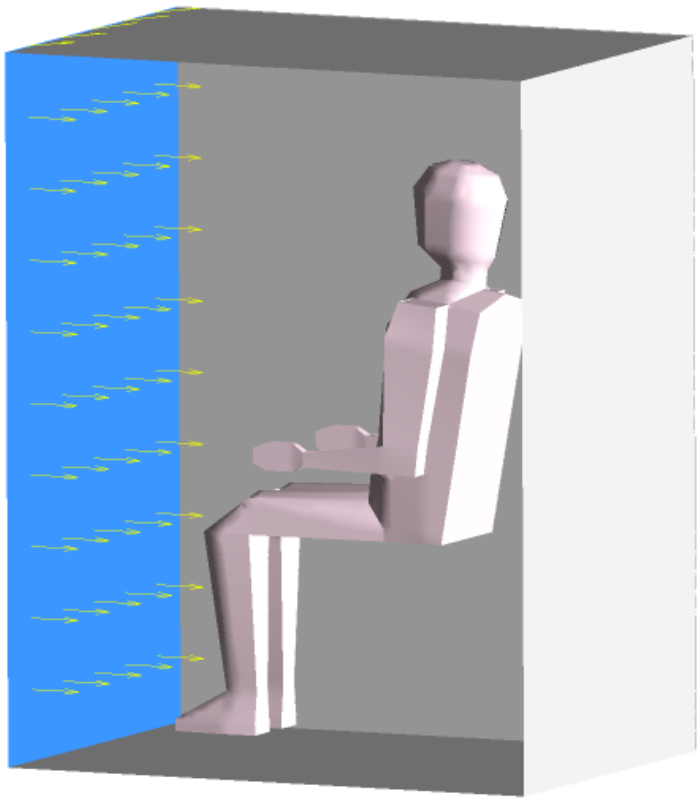

Figure 6.1: Manikin in CFD

The stability of the coupled simulation is mainly influenced by the interval of synchronization and the time constants. The exchanged variables are implemented with a PT1 behavior. So the time constant T is as follows:

$$\frac{dy}{dt} = \frac{ku - y}{T} \tag{6.1}$$

The synchronization time defines the time period after which the variables are exchanged. Higher time constants have no positive impact on the coupling so that it is set to 1 s.

6.4 Results and discussion

In the test cases the first 60 s are calculated in steady state in the CFD calculation. In this case each iteration is handled like a time step. In all cases the time step is set to 0.2 s. After 60 s seconds the simulation is continued in transient mode for 60 s. Figure 6.2 shows the mean skin temperature for a variation of the synchronization time between 0.2 Δs and 20 Δs.

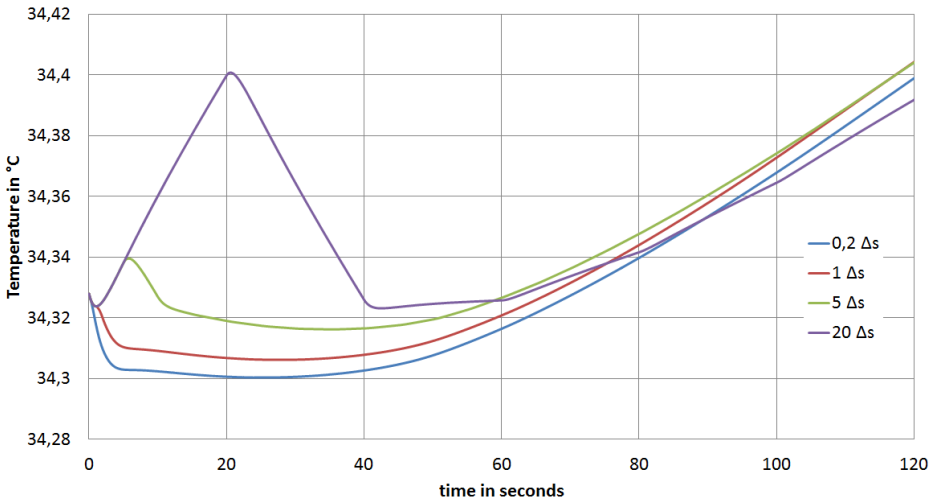

Figure 6.2: Mean skin temperature in CFD

The results show a very smooth change of the mean skin temperature for 0.2 s synchronization time. For an increasing synchronization time bigger temperature jumps occur. It may be expected that those temperature jumps increase in more complex flow fields. So that the according to those results a synchronization time of 0.2 s is recommended.

7 Conclusion

This study solves the problems of perspiration and heat transfer coefficients in the 33 NCM model. Regarding perspiration, is corrected the heat loss by evaporation of sweat, heat production by external work, and the heat balance equation of skin and core layer are now corrected. All the heat transfer coefficients that were constants, now depend on the environmental boundary conditions.

The human physiological system, after all the mentioned improvements works best when the 33 NCM simulates in high temperatures. The perspiration is extremely dependent on the heat transfer coefficients. Consequently a more precise differentiation is necessary in the case of the 33 NCM as a stand-alone tool. All improvements are validated with test cases from the literature. The comparison between simulated results and measurements shows a good correlation for evaporative heat loss or mean skin temperature. Still, rectal and head core temperature is not accurate, in high temperatures. In cold environments the model shows a wrong evolution of body temperatures. If the cooling down of a dead body is well predicted, the wrong behaviour is assumed to be in the active system. As we see, in cold environments, the strongest deviations are located in the shivering, as it might not be predicted correctly. The shivering equation is totally dependent on the head core temperature, that means something is wrong in this equation and needs some future improvements.

Although the 33 NCM model in some cases shows inaccurate values, the tendency is almost always correct, and still has good results for thermal neutrality and even in cold environments is acceptable (except the metabolism). Now the 33 NCM is able to predict values with an excellent accuracy with measurements in a temperature range from 29°C to 48°C, as shown in section 5.3.3 and 5.3.4. When in a neutral environment with temperatures from 25°C to 29°C, the 33 NCM model has good results as shown in section 5.2.2 and 5.2.2. Only under low temperatures as shown in section 5.3.1 and 5.3.2 the 33 NCM does not ensure reliable results, especially if metabolism is analyzed.

This present thesis improves some malfunctions from the 33 NCM, which were discovered in previous studies, but there are still a few more to improve as already found, such as a shivering problem in the metabolism.

Bibliography

Hillel Arkin and Avrahm Shitzer. *Model of Thermoregulation in the Human Body*. Energy Engineering Center, Faculty of Mechanical Engineering, Technion-Israel Institute of Technology, 1984.

ASHRAE. *Thermal Environmental Conditions for Human Occupancy - Standard 55*, volume Thermal Comfort. American Society of Heating, Refrigerating and Air-Conditioning Engineers, Inc., 2013.

Richard J. de Dear, Edward Arens, Hui Zhang, and Masayuki Oguro. Convective and radiative heat transfer coefficients for individual human body segments. *Int J Biometeorol*, 40(141-156), 1997.

T.A. Delchar. *Physics in Medical Diagnosis*, volume Volume 11 of Physics and its applications. Chapman & Hall, 2-6 Boundary Row, 1997.

James D.Hard and Eugene F.DuBois. The technique of measuring radiation and convection. *Journal of Nutrition*, 15:461–475, 1938.

P.O. Fanger. *Thermal Comfort: Analysis and applications in environmental engineering*. New York: McGraw-Hill Book Company, 1970.

M.J. Farabee. The integumentary system, 2010. URL www2.estrellamountain.edu/faculty/farabee/BIOBK/BioBookINTEGUSYS.html.

Dusan Fiala. *Dynamic Simulation of Human Heat Transfer and Thermal Comfort*. PhD thesis, Montfort University, 1998.

J. D. Hardy and J. A. J. Stolwijk. Partitional calorimetric studies of man during exposures to thermal transients. *Journal of Applied Physiology*, 21:1799–1806, 1966.

G. Havenith, I. Holm, E. A. Den Hartog, and K. C. Parsons. *Clothing evaporative heat resistance-proposal for improved representation in standards and models*, volume 43. British Occupational Hygiene Society, 1999.

Charlie Huizenga, Hui Zhang, and Edward Arens. A model of human physiology and comfort for assessing complex thermal environments. *Building and Environment*, 36(6):691–699, 2001.

Frank P. Incropera, Theodore L. Bergman, Adrienne S. Lavine, and David P. Dewitt. *Fundamentals of Heat and Mass Transfer*, volume 7. John Wiley & Sons, Inc., 2011.

Mark Z. Jacobson. *Fundamentals of Atmospheric Modeling*. Stanford University Press, 2005.

Yutaka Kobayashi and Shinichi Tanabe. Development of jos-2 human thermoregulation model with detailed vascular system. *Building and Environment*, 66, 2013.

Clemens Lasance. The thermal conductivity of moist air. *Electronics Cooling*, 2003.

LumaSense Technologies. URL http://www.lumasenseinc.com.

Zoran K. Morvay and Dusan D. Gvozdenac. *Applied Industrial Energy and Environmental Management*. 2008.

Keita Murakami, Shin ichi Tanabe, and Masaoki Haneda. Numerical thermoregulation-model jos for evaluation of thermal comfort. *Proceedings of Roomvent*, 2007.

J. Ostergaard, P.O. Fanger, S. Olesen, and T.H Lund-Madsen. *The effect of man's comfort of a uniform air flow from different directions*, volume 80(2). ASHRAE Transactions, 1974.

Richard Shelquist. An introduction to air density and density altitude calculations, 2012. URL http://wahiduddin.net/calc/density_altitude.htm.

John D. Spengler, Jonathan M. Samet, and John F. McCarthy. *Indoor Air Quality Handbook*. Engineering Handbks, 2000.

J.A.J. Stolwijk and John B. *A MATHEMATICAL MODEL OF PHYSIOLOGICAL TEMPERATURE REGULATION IN MAN*, volume vol. 1855 of *NASA contractor report*. National Aeronautics and Space Administration, 1971.

Rita Streblow. *Thermal Sensation and ComfortModel for Inhomogeneous Indoor Environments*. PhD thesis, RWTH Aachen University, 2011.

Shinichi Tanabe, Kozo Kobayashi, Junta Nakano, Yoshiichi Ozeki, and Masaaki Konishi. Evaluation of thermal comfort using combined multi-node thermoregulation (65mn) and radiation models and computational fluid dynamics (cfd). *Energy and Buildings*, 34:637–646, 2002.

ThermoAnalytics, Inc. URL http://www.thermoanalytics.com.

THESEUS-FE. URL http://www.theseus-fe.com/.

THESEUS-FE. *THESEUS-FE Validation Manual*. P+Z Engineering GmbH, 4.2 edition, June 2012.

Conrad Voelker, Kozo Kobayashi, Junta Nakano, Oliver Kornadt, Edward Arens, Hui Zhang, and Charlie Huizenga. Heat and moisture transfer through clothing. Eleventh International IBPSA Conference, 2009.

XRG Simulation GmbH. URL http://www.xrg-simulation.de.

Hui Zhang. *Human thermal sensation and comfort in transient and non-uniform thermal environments*. PhD thesis, University of California, Berkeley, 2003.